Biosourced Polymeric Emulsifiers for Miniemulsion Copolymerization of Myrcene and Styrene: towards biobased Waterborne Latex as Pickering Emulsion Stabilizer

Maud Save,*[1] Maude Le Hellaye,[1,2] Valentine de Villedon,[1,2] Ismail Adoumaz,[1,3] Marion Pillet,[1] Léonard Atanase,[1] Mohammed Lahcini,[3] Elise Deniau,[1] Abdel Khoukh,[1] Virginie Pellerin,[1] Isabelle Ly,[2] Virginie Dulong,[4] Véronique Schmitt*[2]

[1] Universite de Pau et des Pays de l'Adour, E2S UPPA, CNRS, IPREM, Pau, France.

[2] CRPP, UMR 5031, Univ. Bordeaux, CNRS, 33600 Pessac, France

[3] IMED-Lab, Cadi Ayyad University, Marrakech 40000, Morocco

[4] PBS, Université de Rouen CNRS, 76821 Mont St Aignan.

Corresponding authors: maud.save@univ-pau.fr, veronique.schmitt@crpp.cnrs.fr

† Electronic supplementary information (ESI) available.

Abstract

Biobased waterborne latexes were synthesized by miniemulsion radical copolymerization of biosourced β-myrcene (My) terpenic monomer and styrene (S). Biobased amphiphilic copolymers were designed to act as stabilizers of the initial monomer droplets and the polymer colloids dispersed in the water phase. Two types of hydrophilic polymer backbones were hydrophobically modified by terpene molecules to synthesize two series of amphiphilic copolymers with various degrees of substitution. The first series consists of poly(acrylic acid) modified with tetrahydrogeraniol moieties (PAA-*g*-THG) and the second series is based on the polysaccharide carboxymethylpullulan amino-functionalized with dihydromyrcenol moieties (CMP-*g*-(NH-DHM)). The produced waterborne latexes with diameters between 160 and 300 nm and were composed of polymers with varying glass transition temperatures ($T_{g,\ PMy}$ = - 60°C, $T_{g,\ P(My\text{-}co\text{-}S)}$ = - 14°C, $T_{g,\ PS}$ = 105 °C) depending on the molar fraction of biobased β-myrcene (f_{My},0 = 0, 0.43 or 1). The latexes successfully stabilized dodecane-in-water and water-in-dodecane emulsions for months at all compositions. The waterborne latexes composed of low T_g poly(β-myrcene) caused interesting different behavior during drying of the emulsions compared to polystyrene latexes.

Introduction

Using renewable feedstock as an alternative to fossil feedstock addresses the societal challenge to reduce CO_2-emission. Waterborne latexes are important materials used in the coating industry (decorative paints, inks, adhesives…) and water is used as the continuous phase in their synthesis, which reduces the use of toxic organic solvents. There has been a recent growing interest in the design of biobased waterborne latex by using monomers produced from biomass.[1-9] Biobased stabilizers for oil-in-water emulsions, which are involved in other various fields of applications such as cosmetics, building and agrochemical formulations, also attract increasing interest. Emulsions stabilized by particles, named Pickering emulsions, exhibit remarkable long-term kinetic stability against coalescence thanks to the strong irreversible adsorption of the particles at the oil−water interface.[10, 11] Particles that able to stabilize such emulsions are very diverse in nature ranging from mineral to organic particles and from native to derivatized particles to fully synthetic particles.[12] There has been an increasing interest to use bio-based organic particles in order to improve sustainability of formulations. Examples of such particles are: cellulose nanofibrils or nanocrystals,[13-15] starch granules,[16] dextran nanoparticles,[17, 18] chitosan nanoparticles,[19] and protein nanoparticles.[20] Though various biobased nanoparticles have been used in emulsions,[13, 21-23] so far biobased latex particles have not yet been tested as Pickering emulsifiers. It is therefore of great interest to develop biobased waterborne latexes synthesized by an eco-friendly process as stabilizers of Pickering emulsion. Indeed, polymer latex particles[24-36] or block copolymer latex particles[37] synthesized by emulsion polymerization have also proven to be efficient colloidal particles to stabilize emulsions.

A waterborne latex is a suspension of polymer colloids synthesized by polymerization in aqueous dispersed media. Replacing toxic organic solvent by wateraddresses one of the 12 principles of green chemistry.[38] Using an aqueous phase also reduces the viscosity of final product and improves heat transfer to control polymerization exotherm.[39] Emulsion polymerization is the most widely used process involving a wide range of monomers that can be polymerized by radical polymerization producing polymer particles of *ca* 0.2 to 0.7 µm diameter. Polymerization is initiated by dissociation of the water-soluble initiator (nucleation in the aqueous phase) and proceeds until the polymer chains reach their limit of solubility in water after which they self-precipitate (homogeneous nucleation) or migrate into the core of micelles (micellar nucleation). The polymer particles grow through polymerization fed by diffusion of the monomer through the aqueous phase from dispersed drops of the monomer.

Miniemulsion polymerization has proven to be a suitable method for more hydrophobic monomers containing longer alkyl chain. Miniemulsions contain relatively small monomer droplets produced by high energy input and the polymerization occurs via droplet nucleation.[40, 41] This process is suitable for the hydrophobic monomer produced from biomass feedstock such as vegetable oils or terpenes. In order to produce biobased waterborne latex by (mini)emulsion polymerization, non-water soluble and liquid monomers are required. Different sources of biomass valorized for waterborne latex production have recently been reviewed.[1] It was highlighted that the initial hydrophobic building block most of the time requires a post-derivatization with (meth)acrylic polymerizable groups. Among the various renewable feedstock, we focus our attention here on hydrophobic terpene molecules. Terpenes are C10 or C15 branched or cyclic aliphatic molecules extracted from Pine trees. They are main components of turpentine oil obtained by distillation of gum turpentine or sulfate turpentine, the latter being an inexpensive raw material produced from the Kraft process in paper industry.[42] While several terpenes can be homopolymerized by cationic polymerization, most of the terpenes are not readily homopolymerizable by radical polymerization.[43-46] Some studies reported on the chemical modification of terpenes into (meth)acrylic monomers to produce waterborne latex either by miniemulsion polymerization,[2, 3] or by emulsion polymerization.[4] Unfortunately, chemical derivatization of terpenes often involves hazardous intermediate reactants such as acryloyl chloride[47, 48] or trimethylamine.[2, 49] However, a more recent study attempted to address this problem for terpene-based monomers.[50] On the other hand, terpenes exhibiting a diene structure close to isoprene, the monomer units of polyisoprene present in natural rubber latex, are reactive in radical polymerization without needing any derivatization step.[42, 45] Among this class of terpenes, β-myrcene (7-methyl-3-methylene-1,6-octadiene, Scheme 1) has been by far the most studied dienic terpene for the synthesis of waterborne latex by emulsion polymerization, either homopolymerized[5] or copolymerized with renewable monomers,[6, 7] or with fossil-based methacrylates,[51, 52] or styrene.[53] Polymerization of other dienes like β-farnesene, β-ocimene or allocimene[8, 9] has been less reported. β-myrcene is naturally present at low percentage in number of plants and is produced on a large scale by pyrolysis of β-pinene.[42]

The colloidal stability of a waterborne latex is ensured by repulsive forces, which are either electrostatic, steric or electro-steric. All terpene-based waterborne latexes produced so far were stabilized by conventional fossil-based molecular surfactants.[2, 3, 5-9, 51-53] Also, it is known that the (electro)steric stabilization conferred by macromolecular surfactants, such as

amphiphilic copolymers, is relevant to impart improved stability due to the lower diffusion rate and lower desorption rate of polymers versus molecular surfactants.[54] To the best of our knowledge, no examples of biobased or macromolecular stabilizers have been reported in the literature for the synthesis of terpene-based waterborne latex.

The present work investigates the synthesis of biobased waterborne latex by miniemulsion polymerization stabilized by bespoke macromolecular bioemulsifiers. A biobased hydrophilic backbone (either poly(acrylic acid), PAA, or carboxymethylpullulan, CMP) was derivatized by hydrophobic terpene moieties to produce amphiphilic copolymers (Scheme 1). Since the early patent describing the synthesis of acrylic acid from 3-hydroxypropionic acid produced by fermentation,[55] the industrial production of biobased acrylic acid as monomer for poly(acrylic acid) has raised interest. Carboxymethylpullulan[56] can be produced from pullulan, a natural polysaccharide, with molar masses that make it suitable as stabilizer of polymer colloids (< 20 $kg.mol^{-1}$). The presence of sodium carboxylate groups renders it interesting for electro-steric stabilization. In first instance, the efficiency of the novel biobased comblike amphiphilic copolymers as electro-steric stabilizers for waterborne latex synthesis was investigated using miniemulsion polymerization of styrene that is well-established[41, 57]. Then, increasing fractions of β-myrcene were used to produce either P(S-*co*-My) latexes or fully biobased PMy waterborne latexes stabilized by a terpene-based amphiphilic copolymer. The ability of the presently developed terpene-based waterborne latexes to stabilize dodecane-in-water or water-in-dodecane Pickering emulsions was studied to highlight this functionality. Furthermore, the behavior during emulsion drying was investigated as a function of the β-myrcene fraction with regard to the influence of the latter on the glass transition temperature (T_g) of the polymer.

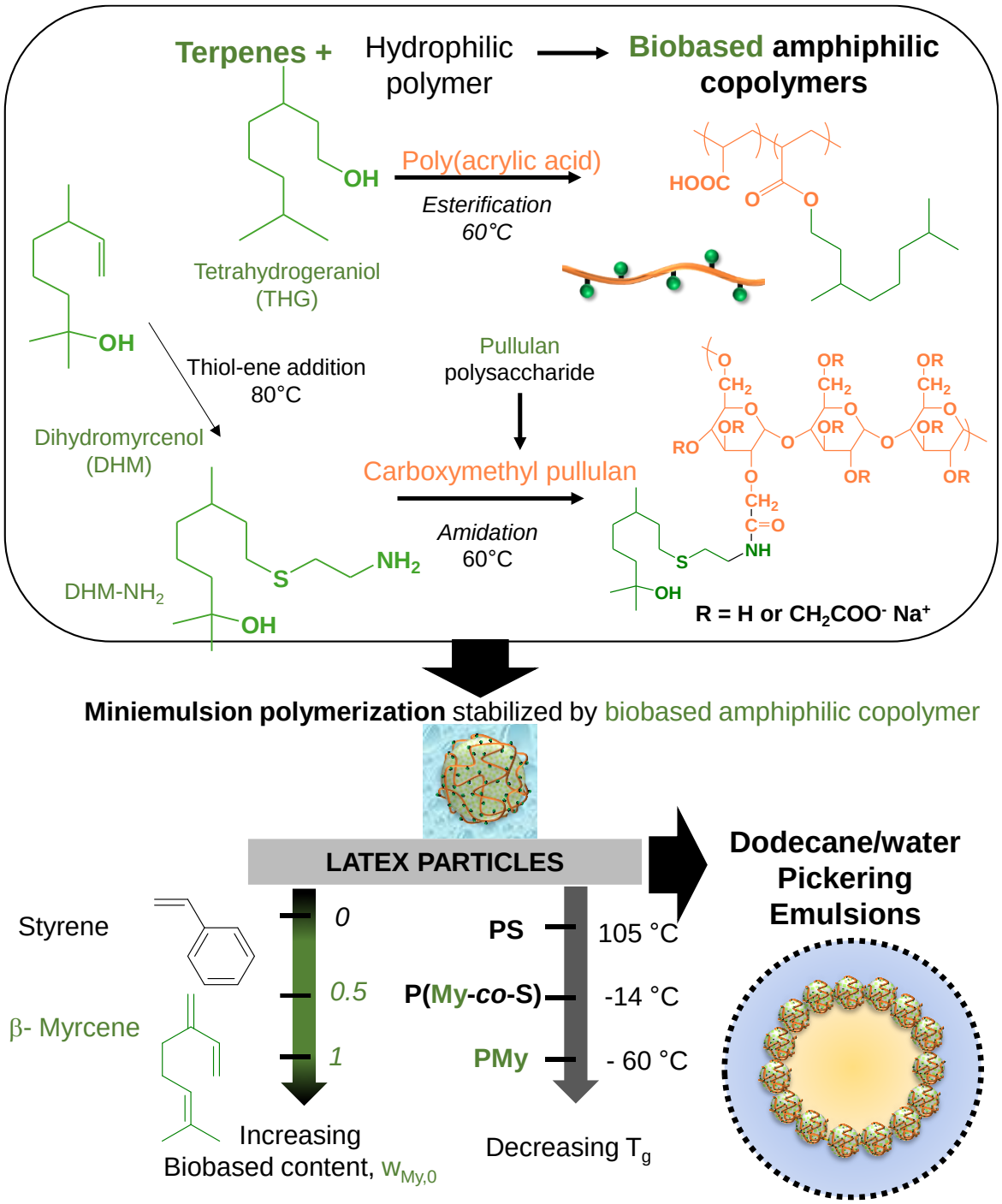

Scheme 1. Synthetic strategy for the synthesis of biobased amphiphilic copolymers used as stabilizers for miniemulsion polymerization producing waterborne latexes with increasing fraction of biobased monomer. Latex particles made of polymer of different T_g are tested as Pickering stabilizers.

Experimental section

Materials. Myrcene (My, 7-methyl-3-methylene-1,6-octadiene) purchased from Sigma-Aldrich (technical grade 80%, stabilized with 1000 ppm butylated hydroxytoluene) was used for all PMy syntheses. According to ^{1}H NMR analysis, this batch of myrcene contains 81

mol-% of β-myrcene and 19 mol-% of α-myrcene (Figure S1). Styrene (S, 99%), tetrahydrogeraniol (THG, 3,7-dimethyl-1-octanol, 98%), cysteamine hydrochloride (98%), sodium borohydride (98%), sodium chloroacetate (98%), 4-(dimethylamino)pyridine (DMAP, 99%), N, N'-dicyclohexyl- carbodiimide (DCC, 98%), 2-2'-Azobis(2-methylpropionitrile) (AIBN, 98%), potassium persulfate (KPS, 99%), hexadecane (99%), sodium bicarbonate powder (99.5%), sodium dodecyl sulfate (SDS, 98%) were purchased from Sigma-Aldrich Merck. Isopropanol (99.5%) and extra dry dimethylsulfoxide (99.7 %, DMSO) over molecular sieve were supplied from Acros Organics. HCl and NaOH solutons were purchased from VWR. Dihydromyrcenol (DHM, 2,6-Diméthyloct-7-ène-2-ol) was supplied by Dérivés Résiniques Terpéniques (DRT, France). Pullulan was purchased from Hayashibara Biochemical Laboratory (Japan).

Synthesis of amphiphilic copolymers and waterborne latexes.

Synthesis of PAA-THG amphiphilic copolymers. The copolymers were synthesized according to the procedure described in our previous work.[58] Poly(acrylic acid) was synthesized by reversible addition fragmentation transfer (RAFT) polymerization and PAA-THG were prepared by esterification of PAA with tetrahydrogeraniol.

Synthesis of CMP-(NH-DHM) amphiphilic copolymers. The first step was the synthesis of carboxymethylpullulan (see details in ESI), as reported elsewhere.[59] The second step required the synthesis of amino-functionalized dihydromyrcenol (DHM-NH_2, Scheme 1) by thiol-ene addition chemistry, which was described in our previous work.[60] CMP-(NH-DHM) amphiphilic copolymers were synthesized by coupling these two precursors as follows. In a 250 mL round bottom flask, CMP in its carboxylic acid form (neutralized CMP passed through ion exchange IRN77 Amberlite cationic resin) was mixed with 20 mL of dry DMSO (0.005% water) and stirred for one hour to completely dissolve CMP. In another flask, 0.191 g of DHM-NH_2 (in the case of an initial molar ratio of DHM-NH_2/carboxylic acid functions = 0.30) was dissolved in 10 mL of DMSO. The two solutions were mixed before adding DCC at a stoichiometric molar equivalent to carboxylic acid functions of CMP and DMAP at 0.4 eq. compared to DCC. The mixture was heated at 60°C for 45 h. In order to stop the reaction, a NaCl solution (3.5 g of NaCl in 30 mL of Milli-Q water) was added to induce the precipitation of the polymer. The polymer was recovered as a white powder by filtration through filter followed by several additions of acetone through the filter.

Synthesis of latex by miniemulsion polymerization. Before polymerization, styrene was mixed for 30 min with an inhibitor remover resin (Sigma Aldrich) to remove *tert*-butylcatechol. The

butylated hydroxytoluene (BHT) inhibitor of myrcene was removed as follows: 8 mL of 1M NaOH solution was mixed with 24 mL of My in a separation funnel. Water was removed and $MgSO_4$ was added to My before being filtered. Inhibitor-free monomers were stored at 4°C. In a typical miniemulsion polymerization for synthesis of PS or P(S-*co*-My) latexes, 100 mg of amphiphilic copolymer (PAA-THG or CMP-(NH-DHM)) was dissolved in 20 g of buffered aqueous solution (0.012 M $NaHCO_3$, pH = 8). In the main round bottom flask, 5 g of monomers (S or S/My) and 280 mg of hexadecane were mixed with 25 mg of AIBN initiator. Aqueous and organic phases were mixed and stirred with a magnetic bar at 300 rpm in an ice bath for 10 min. The emulsion was sonicated with a Branson homogenizer, Ultrasonic Cell Disruptor, SFX550, 13 mm probe, at 30% amplitude for 6 min in an ice bath. A sample was withdrawn as time zero for DLS and conversion measurements before transferring the solution to a 50 mL round-bottom flask. The emulsion was degassed under nitrogen flow for 20 min. The polymerization was then carried out at 70°C for either 6 hours for the polymerization of styrene or for 20 hours for polymerizations involving myrcene. Samples were withdrawn at different time intervals under nitrogen flow in order to determine the monomer conversion by gravimetry. As AIBN was not soluble in myrcene monomer, this initiator was replaced by the water-soluble potassium persulfate (KPS) initiator for My homopolymerization. KPS was added as aqueous solution under nitrogen after the sonication step and before heating up.

Preparation of Pickering emulsions.

Prior to emulsion preparation, each batch of latex particles was washed by successive centrifugation-redispersion cycles in MilliQ water in order to remove any surface-active species. The latex were centrifuged on a Sorvall RC6+ centrifuge at 15400 *g*, where *g* is the terrestrial gravity constant (g = 9.81 m.s^{-2}), at 10°C for 2 h. The particles either creamed (PMy and P(S-*co*-My) latex) or sedimented (PS latex) in the centrifugation tube according to their density (ρ_{PS} = 1.05 g.cm^{-3} and ρ_{PMy} = 0.91 g.cm^{-3}). The surface tension of the super- or sub-natant phase was measured using the pendant drop method. The centrifugation procedure was repeated on average 6 to 10 times until the surface tension of the super- or sub-natant was within ± 1 mN.m-1 from that of pure water (72.8 mN.m^{-1}) (see Figure S2). The Pickering emulsions were prepared as follows: distilled water and the desired mass of washed latex (m_{LW}) were introduced in a flask. Dodecane was added and the bi-phasic liquid mixture was subjected to mechanical stirring with an Ultra Turrax® homogenizer (T25 equipped with IKA® S25N – 25F dispersion probe) operating at 10000 rpm for 30 seconds. The Sauter diameter or surface-average diameter is defined in Eq 1.

$$D_{3,2}=\frac{\sum_i D_i^3}{\sum_i D_i^2}$$

Eq 1

D_i is the diameter of i^{th} droplet and the sum is taken over the total number of observed drops.

Characterization methods.

Size Exclusion Chromatography (SEC). Carboxymethylpullulan was analyzed at 25 °C by size exclusion chromatography (SEC) operating in 0.1 M $LiNO_3$ aqueous eluent filtered through a 0.1 µm filter unit (Millipore, USA) and degassed on-line (DGU-20A3, Shimadzu, Japan) at a flow rate of 0.5 $mL.min^{-1}$. The SEC apparatus is equipped with an automatic injector (SIL-20A Shimadzu, Japan), a OHPAK SB-G guard column for protection and two OHPAK SB 804 and 802.5 HQ columns (Shodex Showa Denko K.K., Japan) in series, a Wyatt Heleos II Multi Angle Laser Light Scattering detector (MALLS, 18 angles, λ_0 = 664.4 nm), a viscometer (ViscoStar II, Wyatt Technology Inc., CA, USA), a SPD-M20A Shimadzu UV-visible detector and a refractive index (RI) detector (RID-10A, Shimadzu). Polymer samples were prepared at concentrations from 3 to 5 $g.L^{-1}$ and filtered through 0.45 µm regenerated cellulose filters. The methylated PAA precursor of PAA-THG were characterized by SEC THF system, which was described along with their synthesis in our previous work.[58]

Fourier transform infra-red spectroscopy (FTIR). The polymers were analyzed as a powder with a spectrometer Nicolet IS50 FT-IR (Thermo Scientific, USA) in attenuated total reflectance mode. The samples were analyzed by transmission from 500 to 4000 cm-1 (128 scan resolution 4) using the OMNIC software.

Proton and DOSY (Diffusion Ordered Spectroscopy) nuclear magnetic resonance. NMR of the copolymers was performed at 25°C on a Bruker Avance 400 spectrometer (400 MHz) (Bruker Instruments). DOSY NMR was performed at 25 °C with a Bruker 5 mm BBFO probe and a gradient amplifier, which provides a z-direction gradient strength of up to 47.5 G cm^{-1}. The temperature was maintained constant within ±0.1 °C by means of a BCU 05 unit. All DOSY NMR experiments were performed using the bipolar longitudinal eddy current delay pulse sequence (BPLED). Typically, a value of 2 ms was used for the gradient duration (δ) 150 ms for the diffusion time (Δ), and the gradient strength (g) was varied from 1.67 $G.cm^{-1}$ to 31.88 $G.cm^{-1}$ in 40 steps. Each parameter was chosen to obtain 95% signal attenuation for

the slowest diffusion species at the last 40th step. The pulse repetition delay (including acquisition time) between each scan was larger than 2 s. Data acquisition and analysis were performed using the Bruker Topspin software (version 2.1). The T1/T2 analysis module of Topspin was used to calculate the diffusion coefficients and to create two- dimensional spectra with NMR chemical shifts along one dimension and the calculated diffusion coefficients along the other.

Dynamic light scattering and zeta potential. The hydrodynamic diameter D_h, polydispersity (PDI) and zeta potential (ξ) of the latex particles were measured by dynamic light scattering (DLS) on a Nano-ZS zetasizer (Model ZEN3600 Malvern Instruments) operating at an angle of 173°. Nano-ZS is equipped with a He-Ne 4.0 mW power laser operating at a wavelength of 633 nm. The particles were dispersed in deionized water at a concentration of 0.05 g.L^{-1}.

Differential Scanning calorimetry (DSC). The glass transition temperature (T_g) of the polymers was measured with a TA Q100 instrument (TA Instruments) under nitrogen flow. For PMy samples, after equilibration at -90°C , samples were heated from - 90°C to 20°C at a rate of 30°C.min^{-1}, then cooled down at the same rate to - 90°C followed by a third heating ramp to measure T_g. For PS samples, heating and cooling ramps between 20°C and 120°C were performed at a rate of 30°C.min^{-1}. The measurement of T_g was performed on the dry extract of latex after water evaporation.

Tensiometry by pendant drop method. Surface tension of supernatants (or subnatants) of centrifuged latex suspensions were measured on a Tracker® hanging-drop tensiometer from Teclis Instruments connected to a computer (acquisition + processing software: WDROP). The solution was introduced into a 100 µL Hamilton glass syringe. A drop was formed in the air, at the end of the needle placed in an optical glass vessel, containing water at the bottom to maintain a constant saturating water pressure. The drop profile was viewed through a camera. The tension was then deduced (by the software) from the axisymmetric drop shape by fitting with the Laplace equation.

Scanning electron microscopy (SEM). Latex particles were metallized with gold to be analyzed on a HIROX SH-3000 microscope at an acceleration voltage of 25 kV.

Atomic Force Microscopy (AFM). All the particles were analyzed on a Bruker Multimode AFM using the PeakForce QNM (r) mode. PeakForce QNM mode is an intermittent contact mode (frequency at 2 kHz) and ScanAsyst-Air tips of very low stiffness (0.4 N.m^{-1}) were used. The data were processed by Nanoscope Analysis software.

Optical microscopy. The emulsions were diluted 10 times in MilliQ water and a small sample of the emulsion was cast on a microscope slide. No upper glass coverslip was used to avoid damaging the droplets. All observations were carried out at ambient temperature on a Zeiss AX10® device, using several objectives (X2.5, X4, X10 and X20). Image acquisition was done with a Hamamatsu camera and uEye software.

Cryo-scanning electron microscopy (Cryo-SEM). The latex particles was imaged with a SEM JSM 6700F Field Emission® from JEOL, connected to a freezing unit and an ALTO 25000® preparation chamber from GATAN. A drop of the sample was cast onto an aluminum holder and frozen by rapid quenching first in liquid propane. The holder was kept under liquid nitrogen then introduced into the preparation chamber. The frozen sample was fractured manually with a scalpel and sublimated at -50°C. After a gold-palladium sputterring, the sample was inserted into the SEM chamber and the stage temperature was kept at -170°C.

Cryofracture preparation and Transmission electron microscopy (TEM). Freeze fracture replica preparation was performed by casting a drop of the sample onto a gold clipboard, then freezing the sample by quickly dipping the holder into liquid propane (cooled through liquid nitrogen). The freezing step must be fast in order to vitrify the sample and avoid structure disruption due to crystallization. Frozen samples were then introduced into the Leica Microsystems BAF 060 freeze-fracture apparatus held at a temperature of - 150 °C and a pressure of 10^{-8} mBar. The samples were fractured using a metal knife held at a temperature of -200 °C. The fractured surface was shadowed by the successive deposition of platinum at an angle of 45° and carbon at an angle of 90°. Outside the BAF060, the gold clipboard was immersed into ethanol to detach the replicas from the samples. Theses replicas were then immersed into several consecutive baths of isopropanol and acetone in order to clean the replica and eliminate any organic residue before observation, and finally in pure water. The replicas were finally collected on 400 mesh copper grids and dried before TEM imaging. Transmission Electron Microscopy was performed with a HITACHI H 600 TEM operating at 75kV.

Results and discussion

Here, miniemulsion polymerization was chosen as polymerization process for several reasons, but mostly because the comblike amphiphilic copolymers used as bio-stabilizers in the present work, do not self-assemble into well-defined micelles, which is required for emulsion polymerization, but do efficiently stabilize monomer-in-water droplets [61-65] that serve as *loci*

of nucleation for miniemulsion polymerization. Ideally, preparation of Pickering emulsions require a post-synthesis washing procedure of latex particles to remove any other surface-active component that could contribute to stabilize the oil/water interface of the Pickering emulsion (see experimental part). For that purpose, centrifugation cycles of particles with diameters above 100 nm are easier than for smaller particles. Since the emulsion polymerization process mainly produced PMy and P(My-*co*-S) latex particles with hydrodynamic diameters in the range of 50 to 80 nm,[5, 53] this process was not considered in the present work. Furthermore, the water solubility of β-myrcene at 20°C ($[My]_{limit\ H2O}$ = 0.005 $g.L^{-1}$) is significantly lower than that styrene ($[S]_{limit\ H2O}$ = 0.240 $g.L^{-1}$), which can affect the relative reactivity in emulsion polymerization due to their different diffusion across the water phase. Copolymerization occurs within the droplets during miniemulsion polymerization, which avoids this issue.

In the following, we will first discuss the efficiency of hydrophobically modified PAA (HMPAA) with tetrahydrogeraniol as the hydrophobic terpene side group for the synthesis of polystyrene, poly(styrene-*co*-myrcene) or polymyrcene waterborne latexes. A second type of biobased amphiphilic copolymer, carboxymethylpullulan derivatized by hydrophobic dihydromyrcenol terpene, is described for the first time to be tested as bio-emulsifier for miniemulsion polymerization of styrene and β-myrcene.

Synthesis of PAA-THG stabilized waterborne latex

The synthesis and characterization of PAA precursors by reversible addition fragmentation transfer (RAFT) polymerization and their derivatization with tetrahydrogeraniol to prepare the PAA-THG amphiphilic copolymers was carried out as described elsewhere.[58, 66] The experimental conditions and the characteristics of the waterborne latex particles that were synthesized are reported in Table 1. The sample names corresponds to the nature of the polymer forming the particles (PS or PMy homopolymers or P(S-*co*-My statistical copolymer) followed by PAA_n-THG_y indicating the macromolecular stabilizer with *n* being the degree of polymerization (DP) of the PAA backbone and *y* being the degree of substitution (DS_{THG}) of PAA in THG.[58] Figure 1 shows that complete conversion of styrene monomers was obtained within 6 hours. As a general trend, varying DP of the PAA backbone from 90 to 345 or increasing DS_{THG} in terpene from 8% to 32% for DP = 180 does not significantly influence the polymerization rate as complete conversion of styrene is reached after 4h for all samples (Figure 1). Miniemulsion polymerization of styrene using 2 wt% of non-derivatized PAA_{180} was carried out under similar conditions as a comparative blank experiment. As a result, the

initial styrene droplets were not well-emulsified as evidenced by the presence of the transparent monomer upper layer after mixing and sonication step (see Figure S3). The final conversion was limited to 68 % of styrene conversion after 6h while conversion was complete by using PAA-THG stabilizer (Table 1). The PAA-stabilized miniemulsion polymerization produced latex with 10 wt-% of coagulum and higher final particle size (D_h = 340 nm). Some few aggregates were observed by DLS and a broad particle size distribution (PDI = 0.2, Figure S3). We think that these results confirmed the added-value of terpene derivatization.

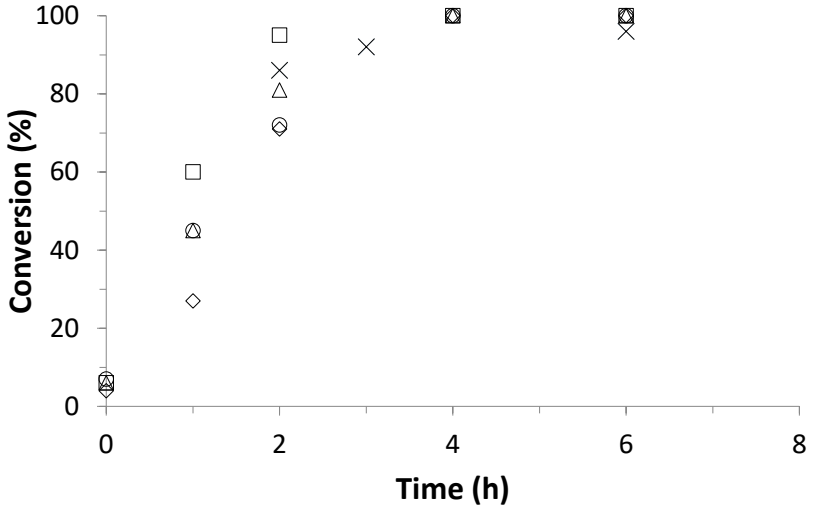

Figure 1. Monomer conversion versus time for styrene miniemulsion polymerization stabilized by 2 wt% of PAA-THG amphiphilic copolymers based on styrene: (□) PAA_{90}-$THG_{0.13}$, (×) PAA_{180}-$THG_{0.09}$, (○) PAA_{180}-$THG_{0.13}$, (△) PAA_{345}-$THG_{0.13}$, (◇) PAA_{180}-$THG_{0.32}$. T_{polym} = 70°C.

Stable monomodal polystyrene latexes were obtained with average hydrodynamic diameters (D_h) ranging between 165 and 315 nm (Table 1). The T_g of polystyrene synthesized by miniemulsion radical polymerization is close to 105 °C (Table S1) so that the integrity of the colloidal polymer particles is maintained upon casting and drying the waterborne latex. This makes it possible to analyze the particles by various microscopy techniques at room temperature. SEM, TEM and AFM images revealed a spherical shape of the PS particles whatever the values of *DP* (n) and DS_{THG} (y) of the PAA_n-THG_y stabilizer (Figure 2a,b,c and Figure S4). Furthermore, all images confirm the narrow particle size distribution of the waterborne latexes that was found with dynamic light scattering in Figure S5. Figure S5 also depicts the stability of the initial liquid miniemulsion of styrene monomer.

a) PS-*stab*-PAA$_{345}$-THG$_{0.13}$ b) PS-*stab*-PAA$_{345}$-THG$_{0.13}$

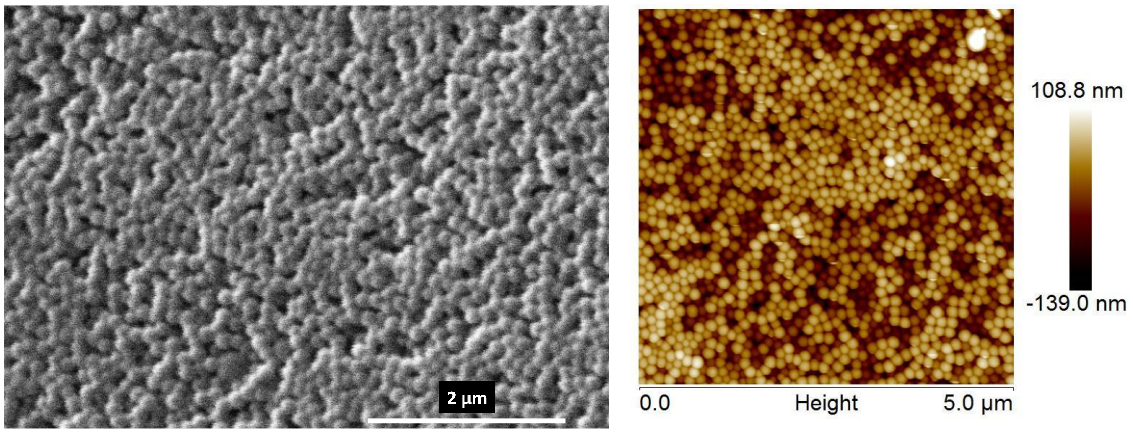

c) PS-*stab*-PAA$_{180}$-THG$_{0.09}$ d) P(S-*co*-My)-*stab*-PAA$_{213}$-THG$_{0.09}$

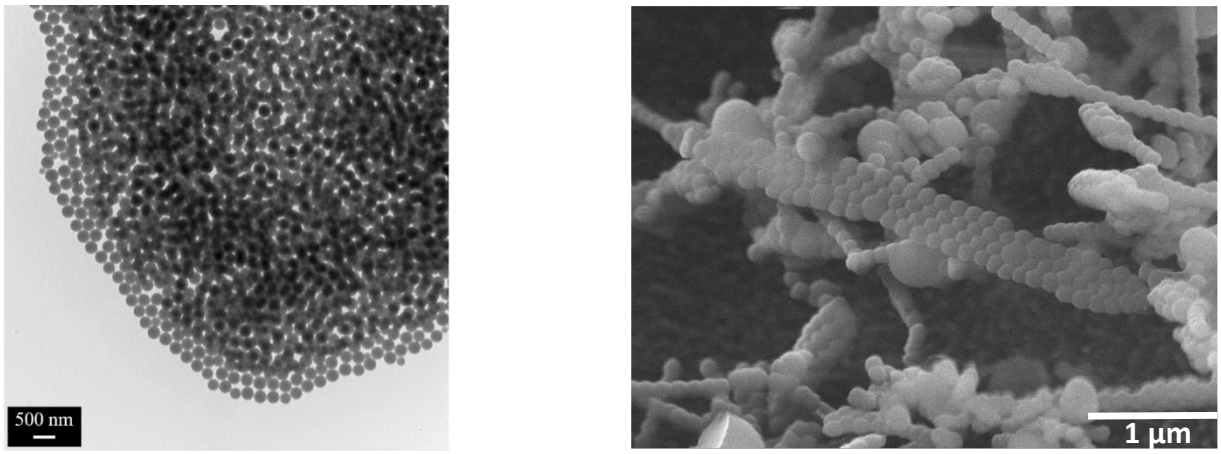

Figure 2. (a) SEM and (b) AFM images (in height of PeakForce QNM mode) of PS-*stab*-PAA$_{345}$-THG$_{0.13}$ latex, (c) TEM image of PS-*stab*-PAA$_{180}$-THG$_{0.09}$ latex (Table 1) and (d) Cryo-SEM image of P(S-*co*-My)-*stab*-PAA$_{213}$-THG$_{0.09}$ latex (Table S4).

Examining the series of PS-*stab*-PAA$_n$-THG$_y$ latex, the average hydrodynamic diameter (D_h) is only slightly modified by varying the DP$_n$ of the PAA backbone in the range of n = 90 to 345 (Figure S5). By using 2 wt-% of the PAA$_n$-THG$_y$ copolymer, the D_h of latex particles were in a similar range for various DS_{THG} above 0.13 but it tends to slightly increase for very low degree of substitution in terpene of y = 0.09 (Table 1). As expected, decreasing the weight fraction of PAA$_n$-THG$_y$ copolymer from 2.0 to 1.4 wt% induced a slight increase of the D_h of PS particles as less interface is stabilized at the initial emulsification step of the monomer droplets and along the course of polymerization (Table 1). A similar trend in colloidal features is observed for the waterborne latexes containing PMy units, see Table 1. Larger D_h were found also for P(S-*co*-My) and PMy particles produced with the smaller

amount of macromolecular stabilizer (1.4 vs 2.0 wt-%) and for PAA_n-THG_y amphiphilic copolymers hydrophobically modified by terpene moieties at a very low extent (DS_{THG} = 0.09).

Table 1. Miniemulsion polymerization of styrene and β-myrcene stabilized by PAA-THG amphiphilic copolymers. T_{polym} = 70°C. The initial monomer content in the aqueous phase is on average 20 wt-%.

f_{My} [a]	w_{My} [a]	Sample Code	Stabilizer (wt.%) [b]	Initiator	$[I]_0$ [c] (mol.L^{-1})	Time (h)	Conv (%)	D_h (nm)	PDI
0	0	PS-*stab*-PAA$_{180}$-THG$_{0.09}$	2.0	AIBN	2.9×10^{-2}	6	100	315	0.12
		PS-*stab*-PAA$_{345}$-THG$_{0.13}$	2.0	AIBN	2.6×10^{-2}	6	100	177	0.08
		PS-*stab*-PAA$_{180}$-THG$_{0.32}$	2.0	AIBN	2.8×10^{-2}	6	100	163	0.12
		PS-*stab*-PAA$_{180}$-THG$_{0.24}$	1.4	AIBN	2.8×10^{-2}	6	83	305	0.30
0.43	0.5	P(S-*co*-My)-*stab*-PAA$_{180}$-THG$_{0.09}$	2.0	AIBN	2.9×10^{-2}	21	40	274	0.08
		P(S-*co*-My)-*stab*-PAA$_{180}$-THG$_{0.32}$	2.0	AIBN	3.0×10^{-2}	24	72	171	0.02
		P(S-*co*-My)-*stab*-PAA$_{180}$-THG$_{0.24}$	1.4	AIBN	2.8×10^{-2}	24	35	254	0.11
1	1	PMy-*stab*-PAA$_{180}$-THG$_{0.09}$	2.0	KPS	1.6×10^{-2}	21	62	250	0.15
		PMy-*stab*-PAA$_{180}$-THG$_{0.32}$	2.0	KPS	1.6×10^{-2}	20	63	236	NA [d]
		PMy-*stab*-PAA$_{180}$-THG$_{0.12}$	1.4	KPS	1.5×10^{-2}	24	29	306	NA [d]

[a] f_{My} and w_{My} are respectively the molar fraction and weight fraction of myrcene in the initial monomer mixture.
[b] Weight fraction of stabilizer with respect to the amount of monomers.
[c] The molar concentration of initiator is calculated with respect to the volume of organic phase (monomer + hexadecane). It corresponds to *ca* 0.5 – 0.6 wt-% of monomers for both AIBN and KPS initiator.
[d] Presence of a second population above 3 µm corresponding to less than 5% in intensity (0% in number). PDI values are provided by the cumulant model, only valid for monomodal size distribution, not applicable (NA) for multi-populated sample.

The introduction of 43 mol% (50 wt%) to 100% of the biobased My monomer in the initial monomer mixture, mainly influenced the propagation rate. While complete conversion of styrene was reached within 6 hours, the monomer conversion remained below 70% after 24 h in the presence of My (Table 1). Note that the presence of 21 mol% α-myrcene isomer (Figure S1), which is less reactive towards radical polymerization, might also be the cause of the incomplete My conversion. Figure 3 shows that increasing the fraction of My monomer led to a decrease of the apparent propagation rate constant (<k_p>), i.e. the slope of Ln([M]$_0$/[M]) *vs* time. This demonstrates the lower reactivity of diene monomers compared to styrene as was already reported for instance by Van Büren *et al.*[67] for isoprene (I) and 1,3 butadiene (Bu) monomers ($k_{p,\ 50°C}$ (I) = 99 L mol^{-1} s^{-1} , $k_{p,\ 50°C}$ (Bu) = 136 L mol^{-1} s^{-1}, $k_{p,\ 50°C}$ (S) = 238 L mol^{-1} s^{-1}). For statistical copolymerization, the average rate constant of propagation (<k_p>) is determined not only by the individual k_p, but also by the reactivity ratios.[68] However, the latter are less important, because the reactivity ratios of styrene and β-myrcene for emulsion radical copolymerization are close (r_{My} = 1.20 and r_S = 0.86).[53] Figure S7 shows a rough estimate of decrease of <k_p> with increasing My molar fraction (f_{My}). It should also be mentioned that the kinetics of miniemulsion homopolymerization of My shown in Figure 3 cannot be directly compared with S and S/My polymerization as the former polymerization was initiated by the water-soluble KPS initiator instead of AIBN. Indeed, AIBN is not soluble in the My monomer droplets. The final composition of the P(S-*co*-My) copolymers was not quantitatively determined by NMR as the P(S-*co*-My) and PMy samples synthesized in the present work had a non-negligible gel content (see Table S1). Crosslinking arose probably from branching reactions due to the presence of unsaturated groups as has been previously discussed for My emulsion polymerization.[5, 9] Owing to the low T_g of P(S-*co*-My) copolymers synthesized by miniemulsion polymerization (T_g ~ - 14 °C < ambient T°) (Table S1), Cryo-SEM was a suitable technique to show that P(S-*co*-My) latex particles also had a spherical shape (Figure 2d).

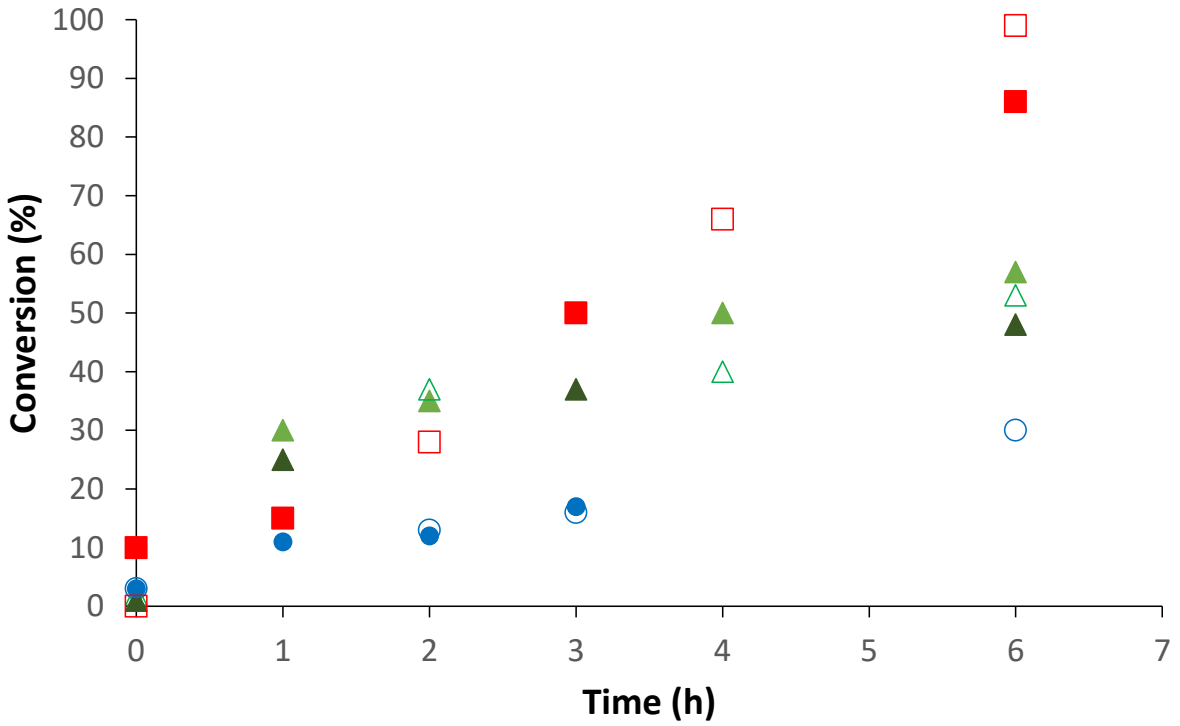

Figure 3. Conversion *vs*. time curves obtained for the miniemulsion polymerization of styrene (red squares) and styrene/myrcene (f_{My} = 0.43) (green triangles) initiated by AIBN or of myrcene (blue circles) polymerization initiated by KPS using various stabilizers: (□) PAA_{180}-$THG_{0.32}$, (■) $(CM_{0.32}P)_{96}$-$(NH\text{-}DHM)_{0.02}$, (△) $(CM_{0.90}P)_{41}$-$(NH\text{-}DHM)_{0.04}$, (▲) $(CM_{0.87}P)_{41}$-$(NH\text{-}DHM)_{0.07}$, (▲) $(CM_{0.30}P)_{96}$-$(NH\text{-}DHM)_{0.04}$, (○) $(CM_{0.84}P)_{41}$-$(NH\text{-}DHM)_{0.10}$, (●) $(CM_{0.90}P)_{41}$-$(NH\text{-}DHM)_{0.04}$, (see Table 1 and Table 3).

The P(S-*co*-My) and PMy waterborne latexes also exhibited a monomodal particle size distribution as displayed in Figure S5. As depicted in Table 1, the hydrodynamic diameters of fully biobased PMy waterborne latexes were between 200 and 300 nm. Some samples contained a very small amount of aggregates (fraction in number is close to zero). As miniemulsion polymerization has often been carried out with conventional fossil-based molecular surfactants such as sodium dodecyl sulfate (SDS), we performed miniemulsion polymerization of S, My and S/My in the presence of SDS (Table S2 and Figure S8) for the sake of comparison with the amphiphilic copolymers. While SDS is clearly a more efficient stabilizer for styrene miniemulsion polymerization initiated by AIBN, it is far less efficient for PMy latex stabilization. Indeed, when using SDS compared to PAA_x-THG_y, the D_h of PS latex was smaller with SDS implying that it better stabilized the interface (Table S2). It is worth noting that a 10 fold decrease of the SDS concentration (from 2 to 0.2 wt% based on styrene) produced PS latex with D_h in the same range as latex stabilized with 2 wt% of

PAA_{345}-$THG_{0.13}$ or PAA_{182}-$THG_{0.32}$ (Table 1 and Table S2). On the other hand, for My miniemulsion polymerization initiated by KPS, unstable latexes were produced by using 0.2 wt% of SDS along with very low monomer conversion (10% after 23 hours), which is characteristic of a poor stabilization. Indeed, 0.5 wt% of SDS allowed only 19% conversion and a fraction of 2 wt% of SDS was required to achieve the synthesis of PMy latex with reasonable My conversion (60%, Table S2) and D_h = 150 nm.

Synthesis of CMP-g-(NH-DHM) stabilized waterborne latex

With the aim of synthesizing biobased amphiphilic copolymers as stabilizers, natural biodegradable and biocompatible polysaccharides emerged as the hydrophilic polymer backbone of choice to design graft amphiphilic copolymers, also named hydrophobically modified polymers (HMP). The modification of polysaccharides by fossil-based alkyl moieties has been extensively reported in the literature. However, as far as we are aware only one study of chemical modification with terpenes as biobased hydrophobic moieties has been reported so far, which focused on the modification of dextran by dihydromyrcenol terpenic groups.[60] Preliminary attempts to use such dihydromyrcenol-derivatized dextran as stabilizer for miniemulsion polymerization of styrene were not convincing with styrene conversions below 60% and a bimodal size distribution of the latexes. Therefore, we used carboxymethylpullulan (CMP), which contains ionized sodium carboxylate groups conferring additional electrostatic stabilization to the steric stabilization offered by hydrophilic non-ionic polysaccharides such as pullulan or dextran.

In the present work, two batches of CMP were synthesized (see Table S3). The first batch $(CM_{0.34}P)_{96}$ had an average molar mass $M_{n,\,CMP}$ = 18300 g.mol^{-1} with a degree of substitution of sodium carboxymethyl groups $DS_{COONa,,CMP}$ = 0.34. The second batch $(CM_{0.94}P)_{41}$ exhibited $M_{n,\,CMP}$ = 9900 g.mol^{-1} and $DS_{COONa,,CMP}$ = 0.94. The dispersity of $(CM_{0.34}P)_{96}$ and $(CM_{0.94}P)_{41}$ was, respectively, 1.12 and 1.36 (Table S3 and Figure S9). The degree of substitution is indicated as x in $(CM_xP)_n$ and corresponds to the number of sodium carboxymethyl groups per anhydroglucosidic unit (AGU). It was determined by conductimetry according to Eq 2, where V_{eq} is the equivalent volume of 0.1 M HCl used for the titration of the weight of neutralized CMP (m_{CMP}), $M_{AGU,\,CMP\ neutralized}$ is the average molar mass of a AGU unit (Eq 3) taking into account the molar mass of pullulan units (162 g.mol^{-1}) and the sodium carboxymethyl groups (80 g.mol^{-1}).

$$x = DS_{\text{COONa, CMP}} = \frac{n_{\text{COOH}}}{n_{\text{AGU,CMP}}} = \frac{V_{\text{eq}} \times [\text{HCl}] \times 162}{m_{\text{CMP}} - (V_{\text{eq}} \times [\text{HCl}] \times 80)}$$

Eq 2

$$M_{\text{AGU, CMP neutralized}} = 162 + 80\ DS_{\text{COONa,0 CMP}}$$

Eq 3

The degree of polymerization (n) of $(CM_xP)_n$ was calculated according to Eq 4 from the number-average molar mass of CMP measured by aqueous SEC MALLS (Table S3 and Figure S8) and of the anhydroglucosidic unit of the neutralized CMP ($M_{\text{AGU, CMP neutralized}}$, Eq 3)

$$n = DP_{\text{CMP}} = \frac{M_{\text{n, CMP}}}{M_{\text{AGU, CMP neutralized}}}$$

Eq 4

Two series of carboxymethylpullulans hydrophobically were modified by terpene groups. The amphiphilic copolymers exhibited various degrees of substitution with hydrophobic dihydromyrcenol pendant chains, DS_{DHM}, ranging between 2 to 10% (Table 2).

Table 2. Summary degree of polymerization and different degrees of substitution of the amphiphilic copolymers based on carboxymethylpullulan (CMP) and dihydromyrcenol (DHM).

Sample Code	$DS_{\text{COONa CMP}}$ [a]	DP_{CMP} [b]	$\frac{n_{\text{DHM,0}}}{n_{\text{AGU, CMP,0}}}$ [c]	DS_{DHM} [d]	$DS_{\text{COONa CMP-DHM}}$ [e]
$(CM_{0.26}P)_{96}$-(NH-DHM)$_{0.08}$	0.34	96	0.30	0.08	0.26
$(CM_{0.30}P)_{96}$-(NH-DHM)$_{0.04}$	0.34	96	0.20	0.04	0.30
$(CM_{0.32}P)_{96}$-(NH-DHM)$_{0.02}$	0.34	96	0.10	0.02	0.32
$(CM_{0.84}P)_{41}$-(NH-DHM)$_{0.10}$	0.94	41	0.36	0.10	0.84
$(CM_{0.87}P)_{41}$-(NH-DHM)$_{0.07}$	0.94	41	0.24	0.07	0.87
$(CM_{0.90}P)_{41}$-(NH-DHM)$_{0.04}$	0.94	41	0.12	0.04	0.90

[a] Degree of substitution in sodium carboxymethyl groups of the initial CMP (Eq 2), which corresponds to the number of groups per anhydroglucosidic unit.
[b] Degree of polymerization of CMP (Eq 4).
[c] Initial ratio between number of moles of DHM-NH_2 (Scheme 1) and number of moles of anhydroglucosidic units of CMP in its carboxylic acid form (Eq 5)

[d] Degree of substitution in DHM-NH pendant chain of CMP-(NH-DHM) copolymer (Eq 6), which corresponds to the number of DHM groups per anhydroglucosidic unit.
[e] Degree of substitution in sodium carboxymethyl of the modified CMP-(NH-DHM): $DS_{COONa,CMP\text{-}DHM} = DS_{COONa\ CMP} - DS_{DHM}$.

The synthesis proceeded through an amidation reaction between CMP in its acidic form and aminoethyl dihydromyrcenol (named DHM-NH_2, see Scheme 1). The synthesis of the DHM-NH_2 intermediate product was carried out by thiol-ene radical addition of cysteamine hydrochloride onto dihydromyrcenol terpene.[60] DS_{DHM} could be tuned by varying the ratio of the initial number of moles of DHM-NH_2 and anhydroglucosidic units of CMP in its carboxylic acid form (Eq 5).

$$\frac{n_{DHM,0}}{n_{AGU,CMP,0}} = \frac{m_{DHM\text{-}NH2} \times (162+59\ DS_{COOH,0})}{M_{DHM\text{-}NH2}\ m_{CMP}}$$

Eq 5

The values of DS_{DHM} reported in Table 2 were determined by ^{1}H NMR by integration of the signal of the anomeric protons of the AGU units and the methyl group of DHM terpenic moiety, see Eq 6 (Figure S10).

$$DS_{DHM} = \frac{(I_{DHM\text{-}NH2})/3}{I_{anomeric\ H}} = \frac{(I_{0.8\text{-}0.9\ ppm})/3}{I_{4.8\text{-}5.6\ ppm}}$$

Eq 6

The ^{1}H NMR signals of CMP AGU units and DHM-NH pendant chains in CMP-(NH-DHM) amphiphilic copolymers were assigned utilizing the individual spectra of each species and literature data (Figure S10).[60, 69] Proton NMR spectra of CMP-(NH-DHM) were recorded for precipitated and purified copolymer (see the experimental section for the purification procedure) to exclude any influence of non-grafted DHM groups in the calculation of DS_{DHM}. DOSY NMR spectra confirmed the efficient grafting as the signal of DHM moieties exhibited similar diffusion coefficients compared to the CMP proton signals (Figure 4).

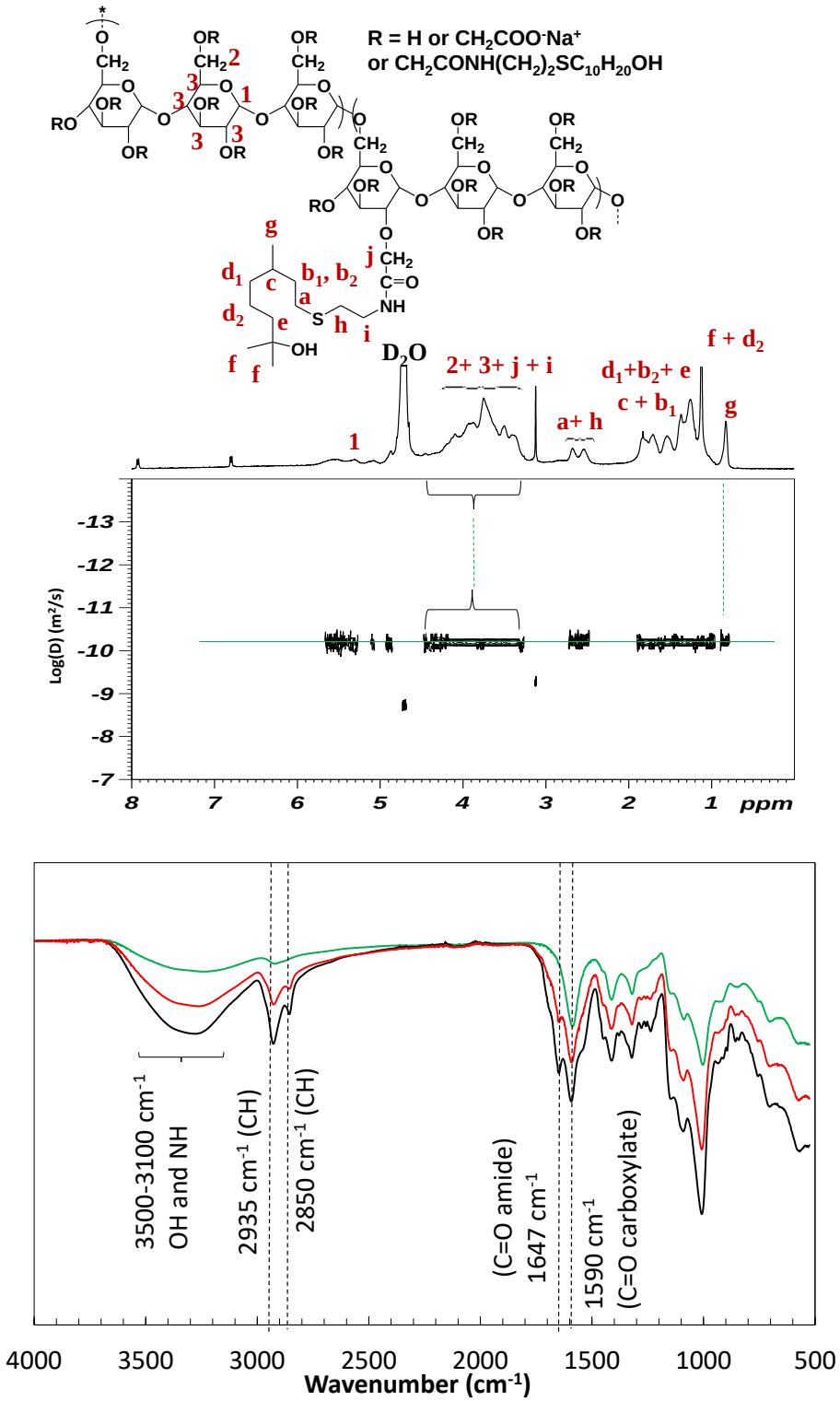

Figure 4. (Top) DOSY NMR spectrum of $(CM_{0.84}P)_{41}$-$(NH\text{-}DHM)_{0.10}$ in D_2O at 25°, (Bottom) Overlay of FTIR spectra of $(CM_{0.90}P)_{41}$ (green line), $(CM_{0.87}P)_{41}$-$(NH\text{-}DHM)_{0.07}$ (red line) and $(CM_{0.84}P)_{41}$-$(NH\text{-}DHM)_{0.10}$ (black line).

The overlay of FTIR spectra of hydrophobically modified CMP-(NH-DHM) with the initial CMP shows the appearance of characteristic signals of the amide band at 1647 cm^{-1} and the

alkyl bands at 2850 cm^{-1} and 2935 cm^{-1} (Figure 4). The increase of the relative intensity of these characteristic FTIR bands by increasing the initial ratio of terpene over AGU units confirms that amphiphilic copolymers with various the degrees of substitution in DHM (Table 2) had been synthesized.

We examined the ability of the CMP-(NH-DHM) amphiphilic copolymers to stabilize waterborne latex synthesized by miniemulsion polymerization of either styrene, β-myrcene or styrene/β-myrcene (with f_{My} = 0.43). We observed similar trends for the polymerization kinetics and impact of the degrees of substitution (DS_{DHM}) as for latex stabilized by PAA-THG. Increasing the fraction of *My* also induced a decrease of the polymerization rate (Figure 3) and required longer polymerization time (Table 3). Despite a lower range of DS_{DHM} compared to DS_{THG}, latexes with hydrodynamic diameters ranging between 200 and 300 nm were produced (Table 3). For polystyrene latex stabilized with CMP with the highest degree of polymerization (PS-*stab*-(CM_xP_{96})-NH-DHM_y)), decreasing DS_{DHM} (= y) from 8% to 2% induced a 20% increase of the particle size. AFM and DLS showed that spherical latexes with a monodal size distribution were obtained (Figure 5 and Figure S11). Thus, CMP-(NH-DHM) amphiphilic copolymers confer a good level of electrosteric stabilization of waterborne latexes in water buffered at pH 7 with $NaHCO_3$. As was found for for PAA-THG, the DP_n of the CMP backbone was not a critical parameter as both P(S-*co*-My)-*stab*-$(CM_{0.30}P)_{96}$-$(NH\text{-}DHM)_{0.04}$ and P(S-*co*-My)-*stab*-$(CM_{0.90}P)_{41}$-$(NH\text{-}DHM)_{0.04}$ latexes were very similar in size and dispersity (Table 2 and Figure S12). Stable PMy latexes were also produced, but PMy latexes stabilized with low hydrophobically modified CMP-based copolymers (DS_{DHM} = 0.04) had a broader particle size distribution (PMy-*stab*-$(CM_{0.30}P)_{96}$-$(NH\text{-}DHM)_{0.04}$ and PMy-*stab*-$(CM_{0.90}P)_{41}$-$(NH\text{-}DHM)_{0.04}$). The results reported in Table 3 show the minor influence of the degree of substitution in ionized sodium carboxylate groups of CMP backbone ($0.3 < DS_{COO^-Na^+} < 0.9$) on latex synthesis.

Table 3. Miniemulsion polymerization of styrene and β-myrcene stabilized by CMP-(NH-DHM) amphiphilic copolymers. T_{polym} = 70°C. The initial monomer content in the aqueous phase is on average 20 wt-% and the weight fraction of stabilizer is 2 wt-% based on monomers.

f_{My} [a]	w_{My} [a]	Sample Code	Initiator	$[I]_0$ [b] (mol.L^{-1})	Time (h)	Conv (%)	D_h (nm)	PDI
0	0	PS-*stab*-$(CM_{0.32}P)_{96}$-$(NH\text{-}DHM)_{0.02}$	AIBN	6.4×10^{-2}	6	86	263	0.43
0	0	PS-*stab*-$(CM_{0.30}P)_{96}$-$(NH\text{-}DHM)_{0.04}$	AIBN	5.9×10^{-2}	6	89	224	0.05
0	0	PS-*stab*-$(CM_{0.25}P)_{96}$-$(NH\text{-}DHM)_{0.08}$	AIBN	5.9×10^{-2}	6	54	225	0.34
0.43	0.50	P(S-*co*-My)-*stab*-$(CM_{0.30}P)_{96}$-$(NH\text{-}DHM)_{0.04}$	AIBN	6.7×10^{-2}	20	80	243	0.09
0.43	0.50	P(S-*co*-My)-*stab*-$(CM_{0.90}P)_{41}$-$(NH\text{-}DHM)_{0.04}$	AIBN	6.9×10^{-2}	20	84	249	0.02
0.43	0.50	P(S-*co*-My)-*stab*-$(CM_{0.87}P)_{41}$-$(NH\text{-}DHM)_{0.07}$	AIBN	6.7×10^{-2}	20	91	293	NA [c]
0.43	0.50	P(S-*co*-My)-*stab*-$(CM_{0.84}P)_{41}$-$(NH\text{-}DHM)_{0.10}$	AIBN	6.5×10^{-2}	20	92	217	NA [c]
1	1	PMy-*stab*-$(CM_{0.30}P)_{96}$-$(NH\text{-}DHM)_{0.04}$	KPS	4.0×10^{-3}	20	42	440/ 83	NA [c]
1	1	PMy-*stab*-$(CM_{0.90}P)_{41}$-$(NH\text{-}DHM)_{0.04}$	KPS	3.9×10^{-3}	22	42	219	0.48
1	1	PMy-*stab*-$(CM_{0.87}P)_{41}$-$(NH\text{-}DHM)_{0.07}$	KPS	3.9×10^{-2}	20	55	243	0.09
1	1	PMy-*stab*-$(CM_{0.84}P)_{41}$-$(NH\text{-}DHM)_{0.10}$	KPS	4.1×10^{-2}	20	63	195	NA [c]

[a] f_{My} and w_{My} are respectively the molar fraction and weight fraction of myrcene in the initial monomer mixture.

[b] The molar concentration of initiator is based on the initial volume of latex (monomers + hexadecane + water). It corresponds to *ca* 0.5 – 0.6 wt-% based on monomers for both AIBN and KPS initiator. My density = 0.79 g.cm^{-3}.

[c] Polydispersity index *(*PDI) is provided by the cumulant model, only valid for monomodal size distribution, not applicable (NA) for multi-populated sample. Presence of a second population above 3 µm corresponding to less than 1-2% in intensity (0% in number) except for PMy-*stab*-$(CM_{0.30}P)_{96}$-$(NH\text{-}DHM)_{0.04}$ sample for which 2 populations were observed at 440 nm (85% in intensity) and at 83 nm (15% by intensity).

The latexes stabilized by CM_xP_n-(NH-DHM)$_y$ are also spherical particles (Figure 5). AFM was suitable to observe PS latex particles, because they have a high T_g and retain their integrity upon drying. AFM images show some segregated nanodomains on the surface of particles that are 5 nm high, 30-45 nm wide and up to 100 nm long (Figure 5 top). These nanodomains are also present on the surface PS-*stab*-PAA-THG latexes (Figure S13 and Figure S14). We suggest that they correspond to aggregates of self-assembled amphiphilic copolymers spread on the surface of particles with terpene pendant chains providing a different response in deformation/adhesion. The PMy-*stab*-(CMP)-(NH-DHM) latex of low T_g (~ -60 °C) exhibit film-forming properties, that are interesting for some coating application, but they limit the observation of the particles in the dried state. TEM images of imprint of PMy-*stab*-$(CM_{0.87}P)_{41}$-$(NH\text{-}DHM)_{0.07}$ latex prepared by cryofracture confirms the spherical shape and, interestingly, shows a surface roughness that may be related to the nanodomains observed by AFM on PS latexes (Figure 5 bottom).

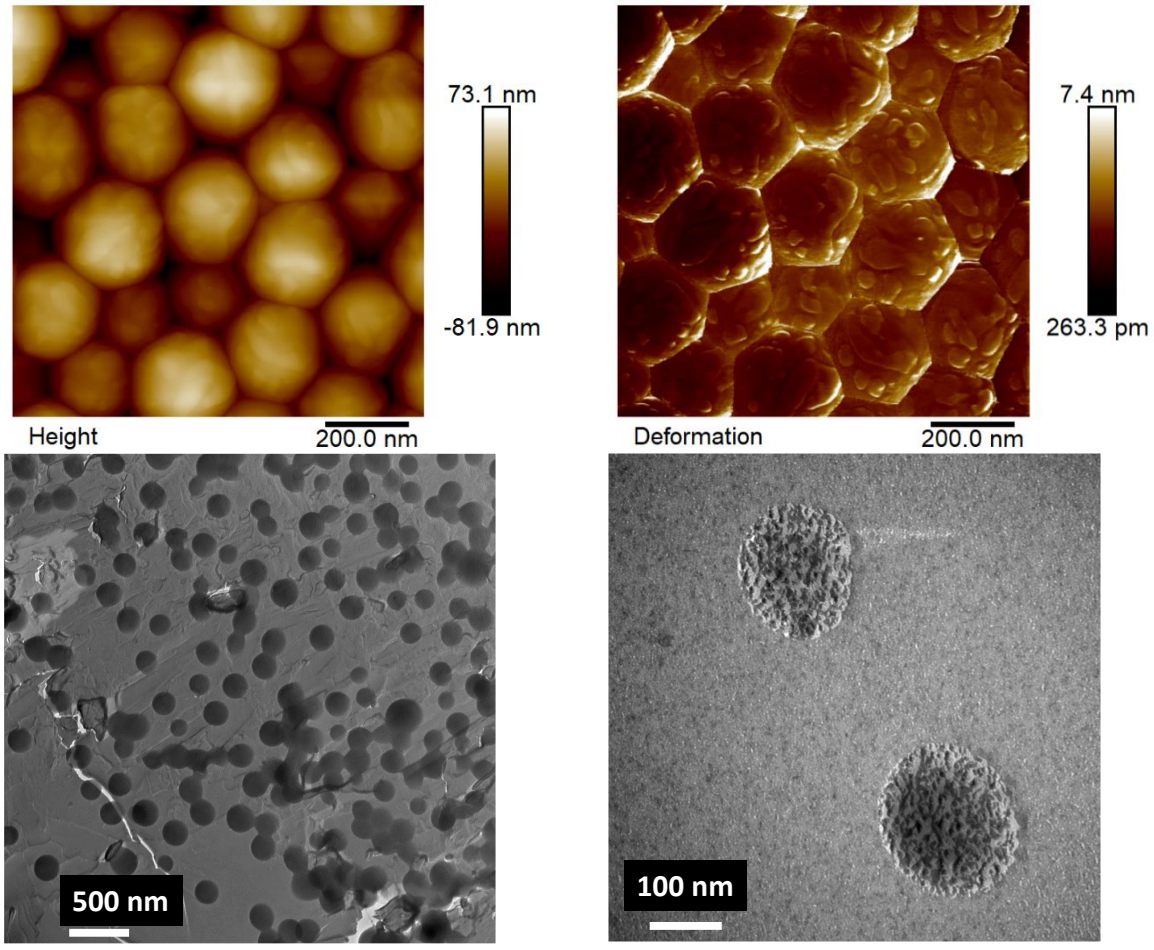

Figure 5. (Top) AFM images (in height or in deformation of PeakForce QNM mode) of PS-*stab*-$(CM_{0.32}P)_{96}$-$(NH\text{-}DHM)_{0.02}$ latex, (Bottom) TEM images of imprint of PMy-*stab*-$(CM_{0.87}P)_{41}$-$(NH\text{-}DHM)_{0.07}$ latex prepared by cryofracture.

As intermediate conclusion, stable waterborne latexes of average diameter of 200 to 300 nm can be successfully synthesized with various fractions of styrene and biobased β-myrcene. Two series of amphiphilic copolymers made with either poly(sodium acrylate) or carboxymethylpullulan as the hydrophilic backbone and hydrophobically modified with terpene moieties areefficient biobased stabilizers for miniemulsion polymerization. Fully biobased latexes were produced in the case of homopolymerization of the β-myrcene terpenic monomer. Thus, a series of polymer particles with a wide range of glass transition temperature (T_g from -60°C to 105°C) covered by two types of anionically charged biobased amphiphilic copolymers was available to be investigated as colloidal stabilizers for Pickering emulsion.

Pickering emulsions stabilized by polymer particles of increasing biobased content

We prepared Pickering emulsions with dodecane, which is not biocompatibility nor of bio-based origin, as a model system. As explained above, any residual species in the water phase that could decrease the surface tension was removed before from the latex particle suspensions. To this end, the latex particles were subjected to several centrifugation cycles until the surface tension of the aqueous supernatant (or subnatant) reached a value close to that of MilliQ water, *ie.* 72.8 ± 1 $mN.m^{-1}$ at 20°C (see Figure and experimental part). The hydrodynamic diameter and zeta potential of the particles were determined after the centrifugation cycles, redispersion and re-concentration. The colloidal features of the particles submitted to centrifugation-redispersion cycles are reported in Table S4. Note that the values of zeta potential of P(S-co-My) latexes synthesized with the AIBN initiator were very close to the ones of PMy latex synthesized with the KPS initiator, hence the number of additional charges brought by the water soluble KPS initiator is low compared to the charges brought by the amphiphilic copolymer. Pickering emulsions were made with six types of latex particles with both types of stabilizers (PAA-THG *vs* CMP-(NH-DHM)) and with different compositions (PS, P(S-*co*-My), PMy). We chose to use equal amounts of dodecane and water so as not to influence the type of emulsion. The dodecane-in-water emulsions and water-in-dodecane are noted as O/W and W/O, respectively, in Table 4. The content of particles, oil and water in the emulsions are summarized in Table 4 as well as the Sauter diameter of the emulsion drops D[3,2].

Table 4. Formulations of Pickering emulsions stabilized by various waterborne latexes. The weight fraction of dodecane and water is 50:50 w:w.[a]

Emulsion	Latex	τ_{WL} (%) [b]	m_L (g) [c]	m_p (g) [c]	w_p (%) [d]	Emulsion type	D[3,2][e] (µm)
E1	PS-*stab*-PAA_{213}-$THG_{0.09}$	5.6	0.79	4.4×10^{-2}	0.22	W/O	236 ± 92
E2	P(S-*co*-My)-*stab*-PAA_{213}-$THG_{0.09}$	3.9	1.15	4.5×10^{-2}	0.22	W/O	27 ± 10
E3	PMy-*stab*-PAA_{213}-$THG_{0.09}$	1.9	9.47	1.8×10^{-1}	0.89	O/W	13 ± 4
E4	PS-*stab*-$(CM_{0.26}P)_{96}$-$(NH\text{-}DHM)_{0.08}$	1.7	4.46	6.9×10^{-2}	0.34	W/O	190 ± 40
E5	P(S-*co*-My)-*stab*-$(CM_{0.87}P)_{41}$-$(NH\text{-}DHM)_{0.07}$	0.5	9.20	4.6×10^{-2}	0.23	W/O	31 ± 18
E6	PMy-*stab*-$(CM_{0.90}P)_{41}$-$(NH\text{-}DHM)_{0.04}$	0.7	6.14	4.3×10^{-2}	0.21	O/W	9 ± 3

[a] The total mass of water includes water coming from the latex suspension and added water is 10 g. The total mass of dodecane is 10 g.
[b] Solids content of the waterborne latex suspension after washing procedure by centrifugation and re-concentration steps.
[c] m_L and m_p are the mass of washed waterborne latex suspension and the mass of polymer particles ($m_p = \tau_{WL}\ m_L$) respectively.
[d] w_p is the weight fraction of particles *vs* total weight of emulsion.
[e] Average surface diameter D[3,2] of the emulsion drops, measured using ImageJ software on an average of 200 drops (for emulsions stabilized by PS or P(S-*co*-My) latexes) and calculated using Eq 1. The error is given by the standard deviation.

Figure 6 displays optical microscopy images of the different emulsions and indicates the type of emulsion. With all latex particles, emulsions were obtained that were stable for at least one year, showing the adsorption and stabilizing ability of the particles. This very high kinetic stability is characteristic for Pickering emulsions.[70] We checked that in the presence of the super-or sub-natant without particles the emulsion were not stable. However, some differences can be observed in Figure 6 and Table 4 between the different systems. With PS and P(S-co-My) particles stabilized with copolymers with a low degree of substitution in hydrophobic terpene, W/O emulsions were formed whereas O/W emulsions were formed with PMy particles. For E1, the drops were very large with a high contrast likely due to a high particle density at the interface. For E4, particles were also visible at the interface even if the contrast was much lower. For this emulsion, the drops exhibited non-spherical shapes revealing the solid behavior of the interface that inhibits shape relaxation. In the presence of β-myrcene (homopolymer or P(S-*co*-My)) in the particles, drops are much smaller (still in the range of ten or several tens of micrometers).

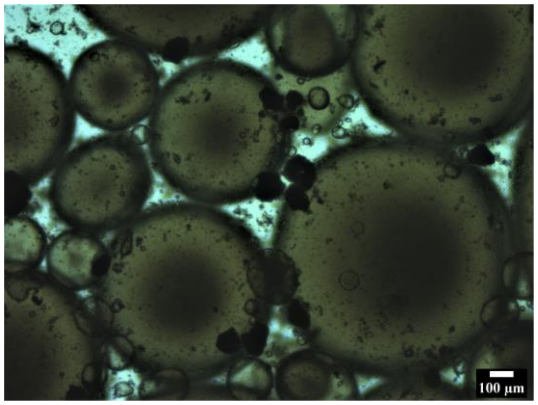

E1: W/O emulsion
PS-*stab*-PAA_{213}-$THG_{0.09}$ latex

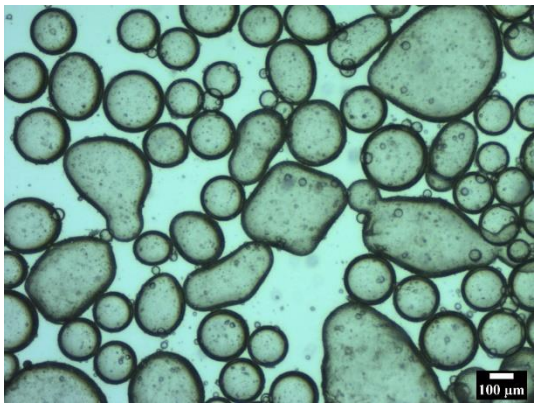

E4: W/O emulsion
PS-*stab*-$(CM_{0.26}P)_{96}$-$(NH\text{-}DHM)_{0.08}$

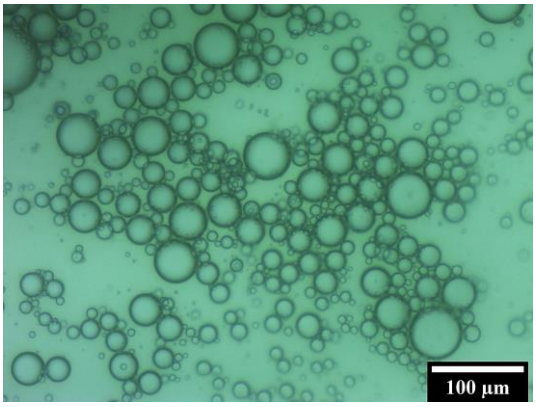

E2: W/O emulsion
P(S-*co*-My)-*stab*-PAA_{213}-$THG_{0.09}$ latex

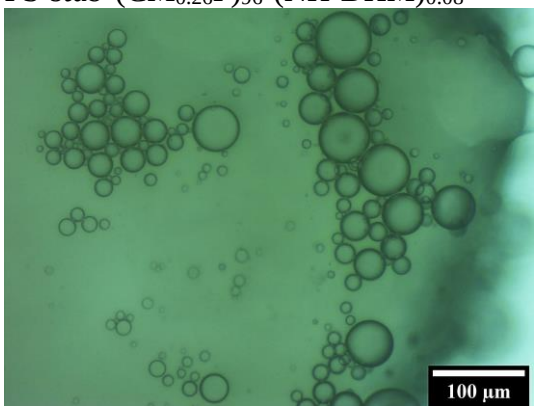

E5: W/O emulsion
P(S-*co*-My)-*stab*-$(CM_{0.87}P)_{41}$-$(NH\text{-}DHM)_{0.07}$

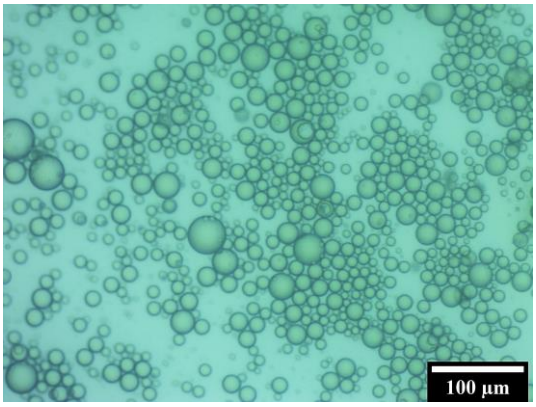

E3: O/W emulsion
PMy-*stab*-PAA_{213}-$THG_{0.09}$ latex

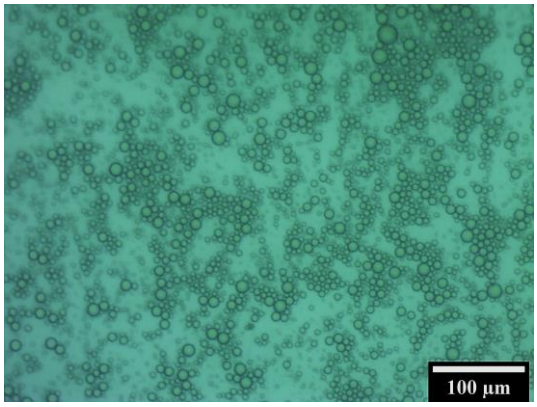

E6: O/W emulsion
PMy-*stab*-$(CM_{0.90}P)_{41}$-$(NH\text{-}DHM)_{0.04}$

Figure 6. Pickering emulsions (containing equal mass of dodecane and water) stabilized by latex particles. Photos of emulsion drops and nature of emulsion (O/W for oil-in-water emulsion and W/O for water-in-oil emulsion). See Table 4 for detailed content of E1 to E6 emulsions.

So far, equal amounts of oil and water were used so as not to influence the type of emulsion. To investigate the impact of the water-oil composition on emulsions stabilized by PMy biobased latex, we prepared a series of four emulsions stabilized by identical PMy-*stab*-PAA_{180}-$THG_{0.27}$ particles, but with various weight fractions of oil, water and particles (Table 5). Figure 7 shows that both E7 and E8 were O/W emulsions evidenced by creaming of the dispersed phase, as for E3 and E6 50/50 w/w emulsions reported in Table 4, while both E9 and E10 were W/O emulsions with dodecane forming a layer top phase.

Table 5 Pickering emulsions stabilized with PMy-*stab*-PAA_{180}-$THG_{0.27}$ particles and various weight fractions of oil (= dodecane), water and particles.

Emulsion	$w_{p/emulsion}$ **(%)** [a]	$w_{p/dispersed\ \varphi}$ **(%)** [b]	w_{H2O} **(%)** [c]	$w_{dodecane}$ **(%)** [c]	**Emulsion Type**	**D[3,2] (µm)** [d]
E7	0.20	0.40	50	50	O/W	304 ± 67
E8	0.55	1.11	50	50	O/W	77 ± 22
E9	0.11	0.40	30	70	W/O	48 ± 17
E10	0.27	1.11	25	75	W/O	14 ± 4

[a] $w_{p/emulsion}$ is the weight fraction of particles *vs* total weight of emulsion.
[b] $w_{p/dispersed\ \varphi}$ is the weight fraction of particles *vs* weight of the dispersed phase.
[c] w_{H2O} and $w_{dodecane}$ are the weight fractions of respectively water and dodecane based on weight of emulsion.
[d] Average surface diameter D[3,2] of the emulsion drops, measured using ImageJ software on an average of 200 drops (for emulsions stabilized by PS or P(S-*co*-My) latexes) and calculated using Eq 1. The error is given by the standard deviation.

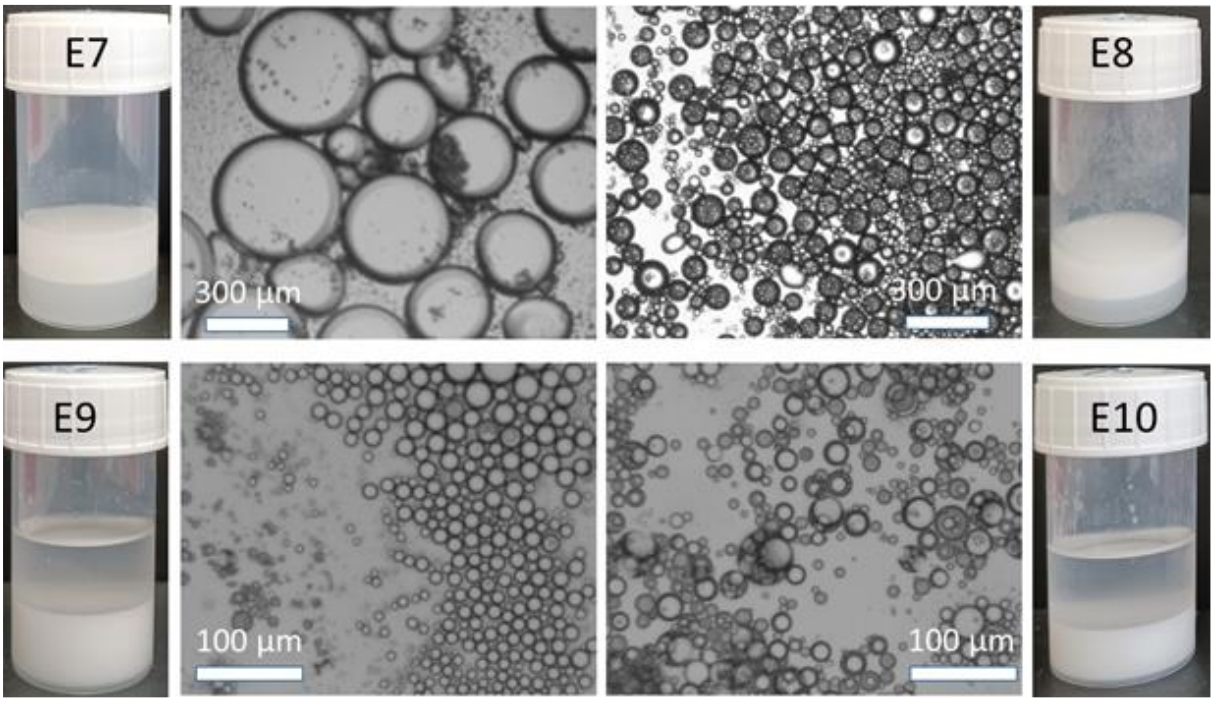

Figure 7. Photography and optical microscopy pictures of Pickering emulsions stabilized by PMy-*stab*-PAA_{180}-$THG_{0.27}$ particles(Top) E7 and E8 are O/W emulsions, (bottom) E9 and E10 are W/O emulsions. (Left) emulsions (E7, E9) with $w_{p/dispersed\ \varphi}$ = 0.4 wt-%), (Right) emulsions (E7, E9) with $w_{p/dispersed\ \varphi}$ = 1.1 wt-% (Table 5).

The dispersed droplets quickly sediment or cream due to their large size and the large difference in density between dodecane and water, which allowed rapid identification of the emulsion type (Figure 7). If the opaque emulsion is located at the top (resp. bottom), it is an oil-in-water emulsion (resp. a water-in-oil)emulsion). It appears that for PMy-*stab*-PAA_{180}-$THG_{0.27}$ particles, the type of emulsion can be tuned by changing the proportion of oil and water, switching from a O/W emulsion for equal weight fractions of oil and water to a W/O emulsion when the oil fractions is above 70 wt-%. This change of emulsion type was not the result of an insufficient amount of particles as the same phenomenon was observed after increasing the amount of particles from 0.4 to 1.1 wt-% (E8 and E10 in Table 5). However, the amount of particles has an impact on the drop size as, whatever the type of emulsion, an increase of the fraction of particles led to a decrease of the surface-average diameter (Table 5). Furthermore, for a given fraction of particles with respect to the dispersed phase, the average drop size was lower for W/O emulsions than for O/W emulsions (E9 *vs* E7 and E10 *vs* E8), possibly due to different particle packing at the interface.

In Pickering emulsions, an increase of the amount of particles may classically induce a decrease of the drop size in the particle-poor regime as a result of the so-called limited coalescence phenomenon.[71] Indeed in this regime, after emulsification, the amount of newly created interface is much larger than the interfacial area the particles can stabilize. As a result, the insufficiently protected drops coalescence until the drop size is adapted to the amount of particles. At higher particle content called particle-rich regime, no more particle amount dependence is observed, the drop size is tuned by the emulsification process. Example of these two regime was observed for other Pickering emulsions.[72] For a constant amount of particles, a catastrophic phase inversion from O/W emulsion to W/O emulsion beyond an oil volume fraction of 0.8 has already been reported for emulsions stabilized by oppositely charged latex particles.[31]

Herein, it appears that the diversity of particles that were synthesized could be used to form emulsions with a variety features (O/W or W/O, with large or small drop sizes) all with a very high stability (Figure S15 Supporting information). As could be expected from the differences in T_g, latexes containing β-myrcene (w_{My}= 0.5 or 1) formed a film upon water evaporation while no continuous film could be seen with PS latexes (w_{My}=0). We then wondered how this difference can be transferred to the emulsions. While no changes with time was observed for all emulsions stored in close vials, we assessed by optical microscopy whether the chemical nature of the particles might affect the evolution of a small amount of emulsion cast onto a glass slide. The results are shown in Figure 8 for two W/O emulsions stabilized by either PS or PMy latexes. Images of drying a O/W emulsion are displayed in Figure S16. The W/O emulsions were diluted with dodecane prior to observation. For emulsion stabilized by PS latex (Figure 8 top, w_{My}=0), it can be seen that the drop volume reduction was almost completely inhibited. Such high resistance to drying has already been observed in Pickering emulsions stabilized by silica particles.[70] This is due to the absence of particle desorption from the interface and from the solid behavior of the interface that exhibits a two-dimensional yield stress.[73] On the other hand, for PMy-stabilized emulsion (Figure 8 bottom, w_{My}=1), the drop volume reduced progressively. The surface became more contrasted (increasing of particle density) and rippling started after 50 min, which is typical behavior of particle-stabilized drops whose surface exhibits rigidity. However, the rigidity did not completely inhibit the drop emptying. The relatively low optical contrast for the crumpled shells remaining in the oil phase arises because there is a relatively small refractive index difference between the copolymer and the oil. The refractive index of dodecane is n = 1.42 and the

refractive indices of common hydrocarbon polymers fall in the narrow range of n = 1.47 - 1.52 (n of PMy is not reported in the literature).[74] At the end, a crumpled shell with a very low optical contrast remained in the oil. Such phenomenon highlighted three features: *i*) particles do not desorb, *ii*) the interface of the drop exhibits rigidity due to the adsorbed particles and *iii)* an almost transparent shell remains. These are the consequences of the irreversible adsorption of particles and solid behavior of the interface able to withstand high stresses, as classically encountered in Pickering emulsions.[73] The different behavior of PMy-stabilized emulsion compared to PS-stabilized emulsion is likely due to the formation of a film as consequence of the low T_g of PMy compared to PS.

To sum up, the chemical nature of the polymer forming the latex particles used as stabilizer governs the different behaviors upon drying the emulsions. The integrity of the polymer shell, formed by the vitrified PS latex particles ($T_{g,PS}$ = 105°C) acting as Pickering emulsifier at the oil/water interface, was maintained upon drying the Pickering emulsion. In contrast, the shell progressively disappeared for PMy-stabilized emulsion thanks to the film-forming property of such latex made of low T_g, polymer ($T_{g,\ PMy}$ = - 60°C). Such behavior could be exploited in future experiments to investigate drying-induced delivery of active molecules.

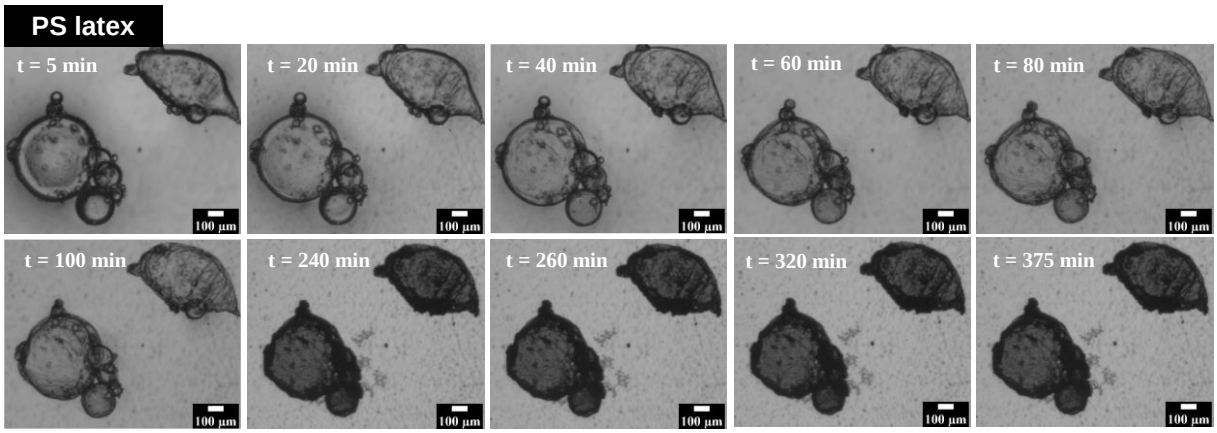

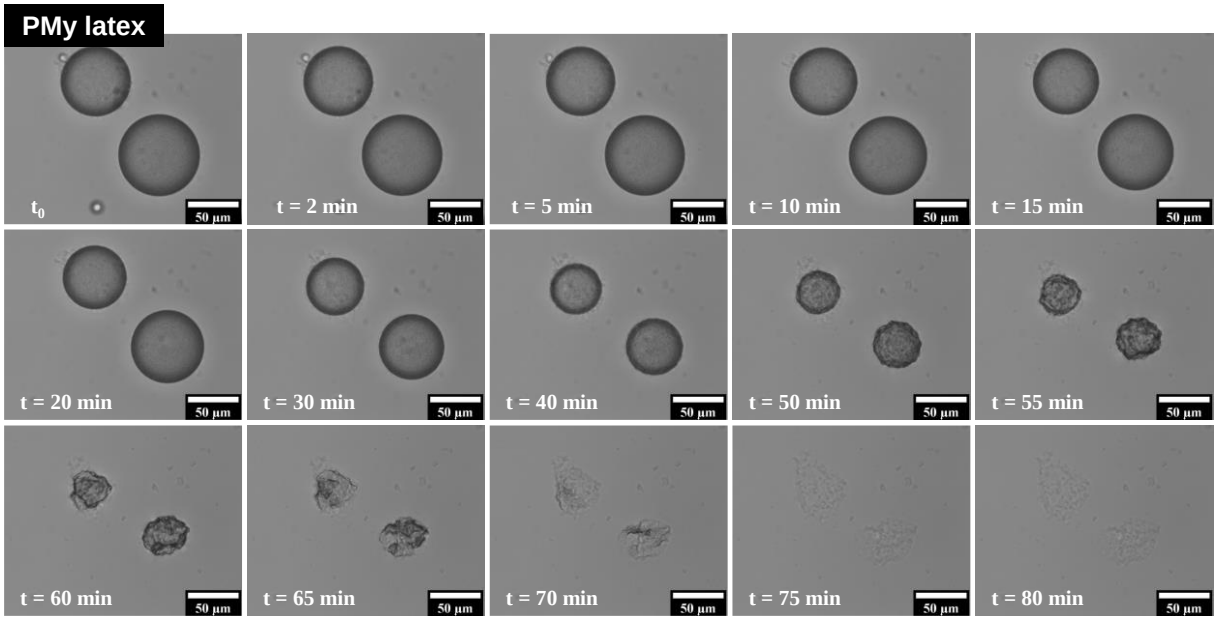

Figure 8. Drying of water-in-dodecane (25/75 w/w) Pickering emulsions at different time intervals. Emulsions stabilized by PS-*stab*-PAA_{180}-$THG_{0.32}$ latex (Top) or by PMy-*stab*-PAA_{180}-$THG_{0.32}$ latex (bottom).

Conclusion

Biobased waterborne latexes can be synthesized by polymerization in aqueous dispersed media using styrene and various fractions of biosourced terpenic monomer, and macromolecular stabilizers from biomass feedstock including terpenes and a polysaccharide or acrylic acid. Miniemulsion polymerization successfully produced stable polyelectrolyte covered latex particles with diameters between 160 and 300 nm, but polymerization rate was lower in the presence of less reactive diene My monomer. Amphiphilic copolymers consisting of hydrophilic backbones (carboxymethyl pullulan or poly(sodium acrylate) hydrophobically modified by terpene grafts are efficient stabilizers. The degree of substitution in terpene, the molar mass and the chemical nature of polymer backbone only slightly influenced the characteristics of the latexes, DS in terpene being the most influencing parameter. Terpene-based waterborne latex can act as effective Pickering stabilizers of oil/water emulsion. In addition to their better sustainability using biobased monomer and stabilizers, this work enables the synthesis of latexes with different T_g, which makes them promising systems for the stabilization of oil/water Pickering emulsions with various properties. Both O/W and W/O emulsions could be stabilized with large or small droplets for durations of more than one year. Finally, the formation of a film at the interface by low T_g biobased poly(β-myrcene) waterborne latexes resulted in interesting behavior upon drying the emulsions.

Associated content

Supporting Information

^{1}H NMR of My, surface tension of supernatants of centrifuged latexes, procedure for the synthesis of CMP, SEM and AFM images of PS latex, auto-correlation functions and particle size distributions of latexes by DLS, droplet size distribution by DLS, estimation of the average constant of copolymerization versus f_{My}, aqueous SEC chromatogram of $CM_{0.94}P$, ^{1}H NMR of $CM_{0.94}P_{41}$ and $(CM_{0.90}P)_{41}$-$(NH\text{-}DHM)_{0.04}$, photo of E3 emulsion over 14 months, optical microscopy of drying of E3 emulsion, T_g values of dried PS, PMy and P(S-*co*-My), experimental conditions and results of latexes stabilized by SDS surfactant, SEC results for 2 CMP, values of D_h, PDI and zeta potential of waterborne latexes after centrifugation cycles.

Conflicts of interest

There are no conflicts to declare.

Acknowledgements

The authors would like to thank Anthony Laffore (IPREM) for support on TGA/DSC. The authors are sincerely grateful to Conseil Regional Nouvelle Aquitaine (CRNA) for funding BIOCOLPIC project and to ADEME for funding ERDG project. The GDR Symbiose is acknowledged for supporting the mobility of Ismail Adoumaz and Valentine De Villedon to LPBS (Université de Rouen). Consortium “Chaire du Pin Maritime” of Bordeaux University is thanked for funding M. Le Hellaye. Campus France is acknowledged for funding Toubkal N° TBK /17/ 51- CAMPUS N° 36877RE project.

References

1. Molina-Gutiérrez, S.; Ladmiral, V.; Bongiovanni, R.; Caillol, S.; Lacroix-Desmazes, P. Radical polymerization of biobased monomers in aqueous dispersed media. *Green Chem.* **2019**, *21*, 36-53.
2. Noppalit, S.; Simula, A.; Billon, L.; Asua, J. M. Paving the Way to Sustainable Waterborne Pressure-Sensitive Adhesives Using Terpene-Based Triblock Copolymers. *ACS Sustain. Chem. Eng.* **2019**, *7*, 17990-17998.
3. Noppalit, S.; Simula, A.; Billon, L.; Asua, J. M. On the nitroxide mediated polymerization of methacrylates derived from bio-sourced terpenes in miniemulsion, a step towards sustainable products. *Polym. Chem.* **2020**, *11*, 1151-1160.

4. Droesbeke, M. A.; Simula, A.; Asua, J. M.; Du Prez, F. E. Biosourced terpenoids for the development of sustainable acrylic pressure-sensitive adhesives: via emulsion polymerisation. *Green Chem.* **2020**, *22*, 4561-4569.
5. Sarkar, P.; Bhowmick, A. K. Synthesis, characterization and properties of a bio-based elastomer: polymyrcene. *RSC Advances* **2014**, *4*, 61343-61354.
6. Sarkar, P.; Bhowmick, A. K. Green Approach toward Sustainable Polymer: Synthesis and Characterization of Poly(myrcene-co-dibutyl itaconate). *ACS Sustain. Chem. Eng.* **2016**, *4*, 2129-2141.
7. Sahu, P.; Bhowmick, A. K. Sustainable self-healing elastomers with thermoreversible network derived from biomass via emulsion polymerization. *J. Polym. Sci., Part A: Polym. Chem.* **2019**, *57*, 738-751.
8. Sahu, P.; Sarkar, P.; Bhowmick, A. K. Synthesis and Characterization of a Terpene-Based Sustainable Polymer: Poly-alloocimene. *ACS Sustain. Chem. Eng.* **2017**, *5*, 7659-7669.
9. Sahu, P.; Bhowmick, A. K. Redox Emulsion Polymerization of Terpenes: Mapping the Effect of the System, Structure, and Reactivity. *Ind. Eng. Chem. Res.* **2019**, *58*, 20946-20960.
10. Pickering, S. U. CXCVI.—Emulsions. *J. Chem. Soc.* **1907**, *91*, 2001-2021.
11. Ramsden, W. Separation of solids in the surface-layers of solutions and 'Suspensions' (Observations on surface-membranes, bubbles, emulsions, and mechanical coagulation). Preliminary Account. *Proc. R. Soc. London* **1903**, *72*, 156-164.
12. Schmitt, V.; Destribats, M.; Backov, R. Colloidal particles as liquid dispersion stabilizer: Pickering emulsions and materials thereof. *C. R. Phys.* **2014**, *15*, 761-774.
13. Kalashnikova, I.; Bizot, H.; Bertoncini, P.; Cathala, B.; Capron, I. Cellulosic nanorods of various aspect ratios for oil in water Pickering emulsions. *Soft Matter* **2013**, *9*, 952-959.
14. Dupont, H.; Laurichesse, E.; Heroguez, V.; Schmitt, V. Green Hydrophilic Capsules from Cellulose Nanocrystal-Stabilized Pickering Emulsion Polymerization: Morphology Control and Spongelike Behavior. *Biomacromolecules* **2021**, *22*, 3497-3509.
15. Dupont, H.; Heroguez, V.; Schmitt, V. Elaboration of capsules from Pickering double emulsion polymerization stabilized solely by cellulose nanocrystals. *Carbohydr. Polym.* **2022**, *279*, 118997.
16. Timgren, A.; Rayner, M.; Dejmek, P.; Marku, D.; Sjoo, M. Emulsion stabilizing capacity of intact starch granules modified by heat treatment or octenyl succinic anhydride. *Food Sci. Nutr.* **2013**, *1*, 157-71.
17. Maingret, V.; Courregelongue, C.; Schmitt, V.; Heroguez, V. Dextran-Based Nanoparticles to Formulate pH-Responsive Pickering Emulsions: A Fully Degradable Vector at a Day Scale. *Biomacromolecules* **2020**, *21*, 5358-5368.
18. Maingret, V.; Schmitt, V.; Heroguez, V. Spatio-temporal control over destabilization of Pickering emulsions stabilized by light-sensitive dextran-based nanoparticles. *Carbohydr. Polym.* **2021**, *269*, 118261.
19. Wei, Z.; Wang, C.; Zou, S.; Liu, H.; Tong, Z. Chitosan nanoparticles as particular emulsifier for preparation of novel pH-responsive Pickering emulsions and PLGA microcapsules. *Polymer* **2012**, *53*, 1229-1235.
20. Paunov, V. N.; Cayre, O. J.; Noble, P. F.; Stoyanov, S. D.; Velikov, K. P.; Golding, M. Emulsions stabilised by food colloid particles: Role of particle adsorption and wettability at the liquid interface. *J. Colloid Interface Sci.* **2007**, *312*, 381-389.
21. Lam, S.; Velikov, K. P.; Velev, O. D. Pickering stabilization of foams and emulsions with particles of biological origin. *Curr. Opin. Colloid Interface Sci.* **2014**, *19*, 490-500.
22. Zembyla, M.; Murray, B. S.; Sarkar, A. Water-in-oil emulsions stabilized by surfactants, biopolymers and/or particles: a review. *Trends Food Sci. Technol.* **2020**, *104*, 49-59.

23. Dupont, H.; Maingret, V.; Schmitt, V.; Heroguez, V. New Insights into the Formulation and Polymerization of Pickering Emulsions Stabilized by Natural Organic Particles. *Macromolecules* **2021**, *54*, 4945-4970.
24. Binks, B. P.; Lumsdon, S. O. Pickering emulsions stabilized by monodisperse latex particles: Effects of particle size. *Langmuir* **2001**, *17*, 4540-4547.
25. Golemanov, K.; Tcholakova, S.; Kralchevsky, P. A.; Ananthapadmanabhan, K. P.; Lips, A. Latex-Particle-Stabilized Emulsions of Anti-Bancroft Type. *Langmuir* **2006**, *22*, 4968-4977.
26. Gautier, F.; Destribats, M.; Perrier-Cornet, R.; Dechezelles, J. F.; Giermanska, J.; Heroguez, V.; Ravaine, S.; Leal-Calderon, F.; Schmitt, V. Pickering emulsions with stimulable particles: from highly- to weakly-covered interfaces. *Phys. Chem. Chem. Phys.* **2007**, *9*, 6455-6462.
27. He, X. D.; Ge, X. W.; Liu, H. R.; Zhou, H. X.; Zhang, Z. C. Self-assembly of latex particles at droplet interface to prepare monodisperse emulsion droplets. *Colloid Surf. A-Physicochem. Eng. Asp.* **2007**, *301*, 80-84.
28. Morse, A. J.; Dupin, D.; Thompson, K. L.; Armes, S. P.; Ouzineb, K.; Mills, P.; Swart, R. Novel Pickering Emulsifiers based on pH-Responsive Poly(tert-butylaminoethyl methacrylate) Latexes. *Langmuir* **2012**, *28*, 11733-11744.
29. Kim, K.; Park, K.; Kim, G.; Kim, H.; Choi, M. C.; Choi, S. Q. Surface Charge Regulation of Carboxyl Terminated Polystyrene Latex Particles and Their Interactions at the Oil/Water Interface. *Langmuir* **2014**, *30*, 12164-12170.
30. Fuma, T.; Kawaguchi, M. Ballooning Behavior of Droplet Sizes in Pickering Emulsions Prepared by Flocculated PS Latexes. *J. Dispersion Sci. Technol.* **2015**, *36*, 1748-1755.
31. Nallamilli, T.; Binks, B. P.; Mani, E.; Basavaraj, M. G. Stabilization of Pickering Emulsions with Oppositely Charged Latex Particles: Influence of Various Parameters and Particle Arrangement around Droplets. *Langmuir* **2015**, *31*, 11200-11208.
32. Binks, B. P. Colloidal Particles at a Range of Fluid-Fluid Interfaces. *Langmuir* **2017**, *33*, 6947-6963.
33. Vasantha, V. A.; Hua, N. Q.; Rusli, W.; Hadia, N. J.; Stubbs, L. P. Unique Oil-in-Brine Pickering Emulsion Using Responsive Antipolyelectrolyte Functionalized Latex: A Versatile Emulsion Stabilizer. *ACS Applied Materials & Interfaces* **2020**, *12*, 23443-23452.
34. Velev, O. D.; Furusawa, K.; Nagayama, K. Assembly of latex particles by using emulsion droplets as templates .1. Microstructured hollow spheres. *Langmuir* **1996**, *12*, 2374-2384.
35. Dinsmore, A. D.; Hsu, M. F.; Nikolaides, M. G.; Marquez, M.; Bausch, A. R.; Weitz, D. A. Colloidosomes: Selectively permeable capsules composed of colloidal particles. *Science* **2002**, *298*, 1006-1009.
36. Yow, H. N.; Routh, A. F. Release Profiles of Encapsulated Actives from Colloidosomes Sintered for Various Durations. *Langmuir* **2009**, *25*, 159-166.
37. Hunter, S. J.; Armes, S. P. Pickering Emulsifiers Based on Block Copolymer Nanoparticles Prepared by Polymerization-Induced Self-Assembly. *Langmuir* **2020**, *36*, 15463-15484.
38. Anastas, P.; Eghbali, N. Green Chemistry: Principles and Practice. *Chem. Soc. Rev.* **2010**, *39*, 301-312.
39. Dube, M. A.; Gabriel, V. A.; Pakdel, A. S.; Zhang, Y. Sustainable polymer reaction engineering: Are we there yet? *Can. J. Chem. Eng.* **2021**, *99*, 31-60.
40. Chern, C. S.; Liou, Y. C.; Chen, T. J. Particle nucleation loci in styrene miniemulsion polymerization using alkyl methacrylates as the reactive cosurfactant. *Macromol. Chem. Phys.* **1998**, *199*, 1315-1322.

41. Asua, J. M. Miniemulsion polymerization. *Prog. Polym. Sci.* **2002**, *27*, 1283-1346.
42. Behr, A.; Johnen, L. Myrcene as a Natural Base Chemical in Sustainable Chemistry: A Critical Review. *Chemsuschem* **2009**, *2*, 1072-1095.
43. Wilbon, P. A.; Chu, F.; Tang, C. Progress in Renewable Polymers from Natural Terpenes, Terpenoids, and Rosin. *Macromol. Rapid Commun.* **2013**, *34*, 8-37.
44. Yao, K.; Tang, C. Controlled Polymerization of Next-Generation Renewable Monomers and Beyond. *Macromolecules* **2013**, *46*, 1689-1712.
45. Satoh, K. Controlled/living polymerization of renewable vinyl monomers into bio-based polymers. *Polym. J.* **2015**, *47*, 527-536.
46. Thomsett, M. R.; Storr, T. E.; Monaghan, O. R.; Stockman, R. A.; Howdle, S. M. Progress in the synthesis of sustainable polymers from terpenes and terpenoids. *Green Mater.* **2016**, *4*, 115-134.
47. Baek, S. S.; Hwang, S. H. Preparation of biomass-based transparent pressure sensitive adhesives for optically clear adhesive and their adhesion performance. *Eur. Polym. J.* **2017**, *92*, 97-104.
48. Noppalit, S.; Simula, A.; Ballard, N.; Callies, X.; Asua, J. M.; Billon, L. Renewable Terpene Derivative as a Biosourced Elastomeric Building Block in the Design of Functional Acrylic Copolymers. *Biomacromolecules* **2019**, *20*, 2241-2251.
49. Sainz, M. F.; Souto, J. A.; Regentova, D.; Johansson, M. K. G.; Timhagen, S. T.; Irvine, D. J.; Buijsen, P.; Koning, C. E.; Stockman, R. A.; Howdle, S. M. A facile and green route to terpene derived acrylate and methacrylate monomers and simple free radical polymerisation to yield new renewable polymers and coatings. *Polym. Chem.* **2016**, *7*, 2882-2887.
50. Droesbeke, M. A.; Du Prez, F. E. Sustainable Synthesis of Renewable Terpenoid-Based (Meth)acrylates Using the CHEM21 Green Metrics Toolkit. *ACS Sustain. Chem. Eng.* **2019**, *7*, 11633-11639.
51. Sarkar, P.; Bhowmick, A. K. Terpene Based Sustainable Methacrylate Copolymer Series by Emulsion Polymerization: Synthesis and Structure-Property Relationship. *J. Polym. Sci., Part A: Polym. Chem.* **2017**, *55*, 2639-2649.
52. Sahu, P.; Sarkar, P.; Bhowmick, A. K. Design of a Molecular Architecture via a Green Route for an Improved Silica Reinforced Nanocomposite using Bioresources. *ACS Sustain. Chem. Eng.* **2018**, *6*, 6599-6611.
53. Sarkar, P.; Bhowmick, A. K. Terpene Based Sustainable Elastomer for Low Rolling Resistance and Improved Wet Grip Application: Synthesis, Characterization and Properties of Poly(styrene-co-myrcene). *ACS Sustain. Chem. Eng.* **2016**, *4*, 5462-5474.
54. Riess, G.; Labbe, C. Block copolymers in emulsion and dispersion polymerization. *Macromol. Rapid Commun.* **2004**, *25*, 401-435.
55. Abraham, T. W.; Allen, E.; Bohnert, E. C.; Frank, C. L.; Hahn, J. J.; Tsobanakis, P. Process for recovery of 3-hydroxypropionic acid from fermentation broth. WO2014144400A1, 2014.
56. Duval, C.; Le Cerf, D.; Picton, L.; Muller, G. Aggregation of amphiphilic pullulan derivatives evidenced by online flow field flow fractionation/multi-angle laser light scattering. *J. Chromatogr. B* **2001**, *753*, 115-122.
57. Landfester, K. Polyreactions in Miniemulsions. *Macromol. Rapid Commun.* **2001**, *22*, 896-936.
58. Atanase, L. I.; Larraya, C.; Tranchant, J. F.; Save, M. Rational design of tetrahydrogeraniol-based hydrophobically modified poly(acrylic acid) as emulsifier of terpene-in-water transparent nanoemulsions. *Eur. Polym. J.* **2017**, *94*, 248-258.

59. Bataille, I.; Huguet, J.; Muller, G.; Mocanu, G.; Carpov, A. Associative behaviour of hydrophobically modified carboxymethylpullulan derivatives. *Int. J. Biol. Macromol.* **1997**, *20*, 179-191.
60. Alvès, M.-H.; Sfeir, H.; Tranchant, J.-F.; Gombart, E.; Sagorin, G.; Caillol, S.; Billon, L.; Save, M. Terpene and Dextran Renewable Resources for the Synthesis of Amphiphilic Biopolymers. *Biomacromolecules* **2014**, *15*, 242-251.
61. Baskar, G.; Landfester, K.; Antonietti, M. Comblike polymers with octadecyl side chain and carboxyl functional sites: scope for efficient use in miniemulsion polymerization. *Macromolecules* **2000**, *33*, 9228-9232.
62. Durand, A.; Marie, E.; Rotureau, E.; Leonard, M.; Dellacherie, E. Amphiphilic polysaccharides: Useful tools for the preparation of nanoparticles with controlled surface characteristics. *Langmuir* **2004**, *20*, 6956-6963.
63. Manguian, M.; Save, M.; Chassenieux, C.; Charleux, B. Miniemulsion polymerization of styrene using well-defined cationic amphiphilic comblike copolymers as the sole stabilizer. *Colloid. Polym. Sci.* **2005**, *284*, 142-150.
64. Durand, A.; Marie, E. Macromolecular surfactants for miniemulsion polymerization. *Adv. Colloid Interface Sci.* **2009**, *150*, 90-105.
65. Obiols-Rabasa, M.; Ramos, J.; Forcada, J.; Esquena, J.; Solans, C.; Levecke, B.; Booten, K.; Tharwat, F. T. Use of Hydrophobically Modified Inulin for the Preparation of Polymethyl Methacrylate/Polybutyl Acrylate Latex Particles Using a Semicontinuous Reactor. *Langmuir* **2010**, *26*, 7717-7724.
66. Atanase, L. I.; Tranchant, J. F.; Gombart, E.; Billon, L.; Save, M.; Alvès, M. H. Amphiphilic acrylic copolymers, process of preparation and uses. WO2016059349A2, 2016.
67. van Büren, B.; Brandl, F.; Beuermann, S. Propagation Kinetics of Isoprene Radical Homopolymerization Derived from Pulsed Laser Initiated Polymerizations. *Macromol. React. Eng.* **2020**, *14*, 1900030.
68. Charleux, B.; Nicolas, J.; Guerret, O. Theoretical expression of the average activation-deactivation equilibrium constant in controlled/living free-radical copolymerization operating via reversible termination. Application to a strongly improved control in nitroxide-mediated polymerization of methyl methacrylate. *Macromolecules* **2005**, *38*, 5485-5492.
69. Glinel, K.; Sauvage, J. P.; Oulyadi, H.; Huguet, J. Determination of substituents distribution in carboxymethylpullulans by NMR spectroscopy. *Carbohydr. Res.* **2000**, *328*, 343-354.
70. Arditty, S.; Schmitt, V.; Giermanska-Kahn, J.; Leal-Calderon, F. Materials based on solid-stabilized emulsions. *J. Colloid Interface Sci.* **2004**, *275*, 659-664.
71. Arditty, S.; Whitby, C. P.; Binks, B. P.; Schmitt, V.; Leal-Calderon, F. Some general features of limited coalescence in solid-stabilized emulsions. *Eur. Phys. J. E* **2003**, *11*, 273-281.
72. Maingret, V.; Chartier, C.; Six, J. L.; Schmitt, V.; Heroguez, V. Pickering emulsions stabilized by biodegradable dextran-based nanoparticles featuring enzyme responsiveness and co-encapsulation of actives. *Carbohydr. Polym.* **2022**, *284*.
73. Arditty, S.; Schmitt, V.; Lequeux, F.; Leal-Calderon, F. Interfacial properties in solid-stabilized emulsions. *Eur. Phys. J. B* **2005**, *44*, 381-393.
74. Jabeen, F.; Chen, M.; Rasulev, B.; Ossowski, M.; Boudjouk, P. Refractive indices of diverse data set of polymers: A computational QSPR based study. *Comput. Mater. Sci.* **2017**, *137*, 215-224.

Table of Content Graphical Abstract